Resonance Broadening of Homogeneous Caesium Vapor in Absorption

Thesis by

Chris Gregory

In Partial Fulfillment of the Requirements for the

Degree of Doctor of Philosophy

California Institute of Technology

Pasadena, California

1941

CONTENTS

Acknowledgements

I wish to express my gratitude to Professor Bowen for rendering much needed encouragement and many helpful suggestions, without which this work would not have been possible. I also wish to thank Professor Houston for his having so kindly discussed the theoretical aspects of the problem. Thanks are also due to Dr. Watanabe for having introduced me to the problem and to Mr. Charles M. Brown Jr. for useful aid in repairing the apparatus.

Abstract

The resonance broadening of homogeneous Cs vapor in absorption was studied by means of the contour method. The intensities were obtained via the method of "astigmatic photometry" by utilizing the astigimatism of the Rowland grating. The pressure of the homogeneous absorbing vapor ranged from 10^{-2} to 17.5 mm Hg. The half breadth varied rather linearly with the number of atoms per unit volume, with $\frac{\gamma_1}{N} \times 10^7 = 1.45$, $\frac{\gamma_2}{N} \times 10^7 = .84$ for the $^2P_{3/2}$ and $^2P_{1/2}$ components of the resonance lines respectively. The average value of the ratio of half breadths γ_1/γ_2 was found to be 1.8. The experimental half width γ is found to be about 1 1/2 times larger than that predicted by Professor Houston. Below pressures of 10 mm Hg the lines exhibited symmetrical broadening according to the "dispersion" formula. At higher pressures indications of a violet and red assymmetry are present for the $^2P_{3/2}$ and $^2P_{1/2}$ components respectively. A definite band on the red side of the $^2P_{3/2}$ and one on the violet side of the $^2P_{1/2}$ was observed.

I. Introduction

The present work is mainly concerned with the shape of the absorption line contours of the resonance lines of homogeneous Cs vapor. In particular, it is wished to ascertain the line contour characteristics as a function of the number of Cs atoms per unit volume within the absorption cell. Now, the work of Lloyd,[1] Watanabe,[2] and Chen[3] with K, Na, and Rb respectively seemed to yield data which were not in complete accord with various theories on line broadening, not to mention the lack of coherence of their respective data. This lack of coherence, then, can be said to be a secondary incentive for the work on Cs. The additional data on Cs is also of importance in the evaluation of current theories[4] on the subject.

Obviously, the non-agreement of theory with experiment and the lack of coherence of the various data can only be resolved by improvements in both theory and experiment. Consequently, an attempt in improving the technique, especially the photographic photometry (the source of an error of approximately 30%) by the autocalibration or astigmatism method[5],[6] is made. In regard to the theory, a somewhat general analysis of the situation on the basis of Dirac's[7] radiation theory is made.

1. Experimental and Theoretical Parameters

Before proceeding further it is well to have in mind the nature and definitions of the quantities involved in the present investigation.

a. Absorption coefficient: α_ν

First of all the absorption coefficient which is usually denoted

by α_ν is defined to be

$$\alpha_\nu \equiv \frac{-d \log_e i_\nu}{dx} \quad 8) \qquad (1)$$

where di_ν is the intensity of radiation of frequency ν withdrawn from the radiation of intensity i_ν when it traverses a path length dx. If α_ν is not a function of path length (1) is equivalent to

$$i_\nu = i_0 e^{-\alpha_\nu x} \qquad (2)$$

where i_0 is the incident intensity of radiation on a slab of thickness x and i_ν is the intensity which emerges. i_0 and i_ν represent the amount of energy which passes perpendicularly through unit cross section in unit time.

b. Intensity of Absorption A_ν

On the other hand the intensity of absorption A_ν at frequency at frequency ν is defined as the energy absorbed per unit cross section in unit time by a slab of thickness x:

$$A_\nu = i_0(1 - e^{-\alpha_\nu x}) \qquad (3)$$

One concludes, then, that when $\alpha_\nu x \prec\prec 1$, $A_\nu \cong i_0 \alpha_\nu x$.

c. Intensity Distribution $I(\nu)$. Half Breadth $\Delta\nu_{1/2}$

$I(\nu)$, the intensity distribution of a broadened absorption line is defined to be proportional to α_ν the absorption coefficient:

$$I(\nu) \propto \alpha_\nu \qquad (4)$$

As we see from (3) the physical significance of $I(\nu)$ is as follows: It is merely proportional to the intensity of absorption A_ν for the case of an infinitely thin sheet of absorbing atoms.[9] It is found convenient to normalize the intensity distribution so that

$$\int_0^\infty I(\nu)d\nu = 1 \tag{5}$$

In case $I(\nu)$ is a function symmetric about $\nu = \nu_0$ at which frequency $I(\nu)$ is a maximum, then a convenient characteristic of the absorption line, $\Delta\nu_{1/2}$, the so-called half breadth is defined by the following equation

$$I(\nu_0 \pm \frac{1}{2}\Delta\nu_{1/2}) = \frac{1}{2} I(\nu_0) \tag{6}$$

It may so happen that $I(\nu)$ is not symmetrical about $\nu = \nu_0$, say. In this case no satisfactory quantity has been found to characterise the distribution $I(\nu)$. Several suggestions have been proposed[10] but it is doubtful that these are of much use. In the final analysis $I(\nu)$ for every ν must be known.

d. Correlation of Einstein Coefficient B_{ij}, f-values and α_ν

It has been shown[11] that the Einstein coefficient of absorption B_{ij} is connected with the α_ν in the following manner:

$$B_{ij} = \frac{c}{h\nu_{ij}N} \int_{\text{Over line}} \alpha_\nu \, d\Delta\nu \tag{7}$$

where c is the velocity of light, h Planck's constant, ν_{ij} the frequency

and N the number of atoms per unit volume. (7) is valid when the Boltzmann factor can be neglected which is usually the case. Furthermore the so-called f-value or oscillator strength is defined[12] as

$$f_{ji} \equiv \frac{B_{ij} mh \nu_{ij}}{\pi e^2} \tag{8}$$

m being the mass of an electron and e its charge in e.s.u. For experimental and calculated f-values a useful summary is given by Korff and Breit[13]. (7) and (8) enables one to ascertain the constant of proportionality in (4).

2. Theoretical Review

No attempt will be given in this section to derive expressions descriptive of the phenomenon of line broadening. Nevertheless, a qualitative discussion of the situation will be given. For more details the reader is referred to the literature on the subject. In classifying the various causes for the broadening of spectral lines the following summary is convenient:

- 2 a. Natural Damping
- 2 b. Doppler Broadening
- 2 c. Mutual Influences of Atoms
  - i. Lorentz Collision Broadening
  - ii. Broadening and Displacement Due to Force Fields of Neighboring Atoms

2 a. Natural Broadening

On the basis of the classical theory each spectral line emitted from a body was supposed to be associated with the radiation emitted by so-called "virtual oscillators" within the body which consisted of elastically bound electrons. Starting with such a model it was possible to obtain an expression indicative of the finite breadth of spectral lines after invoking the results of electromagnetic theory. In essence the natural broadening was explained by the fact that an accelerated electron continuously emits energy which has the effect of damping its motion, and which in turn gives rise to the finite line breadth that the virtual oscillator emits or absorbs.[14] It is well to note that in the case of a sufficiently dilute gas in a container the damping is to a large extent electromagnetic in nature so that even an isolated atom in the process of emission or absorption exhibits continuous absorption or emission. The upshot of the situation is that the intensity distribution becomes

$$I(\nu) = \frac{\gamma}{2\pi} \frac{1}{(\nu - \nu_0)^2 + (\frac{\gamma}{2})^2} \tag{1}$$

where ν_0 is the frequency that would be emitted or absorbed when the radiation damping is ignored. By I (6) and the relation $c = \lambda\nu$ the half breadth due to natural damping is

$$\Delta\nu_{1/2} = \frac{\gamma}{2} \tag{2}$$

which turns out to be in terms of wave length

$$\Delta\lambda_{1/2N} = \frac{4\pi}{3}\frac{e^2}{mc^2} = 1.17 \times 10^{-4}\ \text{Å} \quad (3)$$ [15]

which is a universal constant independent of the frequency ν_0. Consequently, according to the classical theory all absorption or emission lines should have the same breadth.[16] The quantum theory contradicts this assertion.

Now, in quantum mechanics the natural breadth arises from the fact that each of the two energy levels between which a transition takes place are not infinitely sharp but have a finite breadth, say, ΔE_1 and ΔE_2. According to the theoretical considerations of Weiskopf and Wigner,[17] and Hoyt[18] the intensity distribution within a line is given by

$$I(\nu) = \frac{\gamma}{2\pi}\frac{1}{(\nu_{21}-\nu)^2 + \left(\frac{\gamma}{2}\right)^2} \quad (4)$$

which is essentially the same as that given (1) but with the important difference that

$$\gamma = \gamma_1 + \gamma_2 = \frac{\Delta E_1}{h} + \frac{\Delta E_2}{h} \quad (5)$$

where γ_1 and γ_2 are the term widths of the two levels between which a transition occurs. In fact the quantum theory maintains that $\gamma_i = \sum_{j<i} \omega_{a_i a_j}$ where $\omega_{a_i a_j}$ represents the transition probability for the transition $a_i \rightarrow a_j$. The breadth of a certain line say $a_i \rightarrow a_k$ is then

$$\gamma_{ik} = \gamma_i + \gamma_k \quad (6)$$

In terms of the so-called f values we may write

$$\gamma_i = \frac{4\pi e^2}{mc^3} \sum_{j<i} \frac{g_j}{g_i} \nu_{ij}^2 f_{ij} \qquad (7)$$

where g_k is the statistical weight of the level $k : (2J_k + 1)$ and f_{ij} is the number of dispersion electrons for the transition $i \rightarrow j$. This latter quantity is a hangover from the classical theory of dispersion where it represented the ratio of the number of quasi-elastically bound electrons to the total number. It was found to be constant for a particular line. ν_{ij} is, of course, the frequency for the transition $i \rightarrow j$. In the quantum theory, f in the case of a simple resonance line is inversely proportional to the lifetime of the resonance level. From (7) and (6) we can then write for the half breadth:

$$\Delta\nu_{1/2}\, i \rightarrow j = \gamma_{ij} =$$

$$\frac{4\pi e^2}{mc^3}\left[\sum_{j<i} \frac{g_j}{g_i} \nu_{ij}^2 f_{ij} + \sum_{\ell<k} \frac{g_e}{g_k} \nu_{ke}^2 f_{ke} \right] \qquad (8)$$

If one is considering a resonance line $i \rightarrow k$, where i is the ground state (8) becomes

$$\Delta\nu_{1/2}\, i \rightarrow k = \frac{4\pi e^2}{mc^3} \frac{g_i}{g_k} \nu_{ki}^2 f_{ki} \qquad (9)$$

The above results can be understood in the light of Heisenberg's uncertainty relation for energy and time

$$\Delta E \Delta t \geqq \hbar \qquad (10)$$

where ΔE is the uncertainty in the energy of the system and Δt is the time available for measuring the energy. The excited state of the atom has a life time γ^{-1}; consequently, the energy of the excited state is uncertain to the extent $\Delta E = \hbar\gamma$, whence the finite breadth. Similar considerations give when several atomic states exist expressions like (6) or (8). Since if we have two terms E_1 and E_2 each uncertain to extent ΔE_1 and ΔE_2 and furthermore if the term values are distributed according to

$$I_1(E) = \frac{\Delta E_1}{2\pi} \frac{1}{(E - E_1)^2 + (\frac{\Delta E_1}{2})^2}$$

and

$$I_2(E) = \frac{\Delta E_2}{2\pi} \frac{1}{(E - E_2)^2 + (\frac{\Delta E_2}{2})^2} \qquad (7)$$

then by the multiplication law of probability for two independent events the combined distribution can be represented as

$$I_{1+2} = \int_0^\infty I_1(E') I_2(E' - E) dE' \qquad (8)$$

Putting (7) in (8) and integrating (using residue theory) it can be readily shown that

$$I_{1+2}(E) = \frac{\Delta E_1 + \Delta E_2}{2\pi} \frac{1}{(E - E_{12})^2 + (\frac{\Delta E_1 + \Delta E_2}{2})^2} \qquad (9)$$

Distributions like (1), (4) and (7) exhibit the property (9). In the literature such distributions are called "dispersion" distributions.

2 b. Doppler Broadening

If an atom is moving linearly with a velocity v and is in the process of emitting or absorbing light of frequency ν_0 the frequency appears to be displaced by the amount

$$\Delta\nu = \pm \nu_0 \frac{\xi}{c} \tag{10}$$

where ξ is the component of v in the direction of observation. If one makes use of the Maxwell-Boltzmann distribution law the intensity distribution due to this cause becomes

$$I(\nu) = \left(\frac{MC^2}{2\pi RT\nu_0^2}\right)^{\frac{1}{2}} \exp + \frac{-MC^2}{2RT\nu_0^2}(\nu - \nu_0)^2 \tag{11}$$

Whence from I (6) we have

$$\Delta\nu_{1/2} = 2(\ln 2)^{\frac{1}{2}} \left(\frac{2RT}{MC^2}\right)^{\frac{1}{2}} \nu_0$$

or
$$\Delta\lambda_{1/2} = 2(\ln 2)^{\frac{1}{2}} \lambda_0 \left(\frac{2RT}{MC^2}\right)^{\frac{1}{2}} \tag{12}$$

where R is the gas constant, M the mass of the atom and T the absolute temperature. At ordinary temperatures the natural breadth and the Doppler breadth are of the same order of magnitude when $\lambda \simeq 100$ Å. Above this the Doppler, and below the natural breadth is predominant. On the other hand, at the wings of the line of the combined effect the natural breadth distribution (1) or (4) holds yet - since the Doppler distribution dies down much more rapidly than the dispersion type of

distribution.

To obtain the combined Doppler-Damping broadening one reasons as follows:[19] Because of the motion of the atom, the center of the damping distribution is no longer at ν_o but is displaced by an amount $\Delta = \xi\nu/c$. The center is now at $\nu_o + \Delta$. But the probability that the center is displaced between Δ and $\Delta + d\Delta$ is $\exp - \Delta^2/b^2\, d\Delta$, hence the resulting damping + Doppler distribution is

$$I_{N+D}(\nu) = \frac{\gamma}{b\pi^{3/2}} \int_{-\infty}^{+\infty} \frac{\exp -\Delta^2/b^2\, d\Delta}{(\nu - \nu_o - \Delta)^2 + (\gamma/2)^2} \tag{13}$$

where

$$b = \frac{\nu_o}{c}\left(\frac{2RT}{M}\right)^{\frac{1}{2}} \tag{14}$$

For distances far removed from the center of the line (13) becomes

$$I(\nu - \nu_o) = \frac{\text{Const}}{(\nu - \nu_o)^2 + (\frac{\gamma}{2})^2}\left[1 + \frac{3}{2}\frac{b^2}{(\nu - \nu_o)^2 + (\frac{\gamma}{2})^2} + \cdots\right] \tag{15}$$

Hence when $(\nu - \nu_o)^2 + \gamma^2/4 >> b^2$ we have essentially the damping distribution. Even when $(\nu - \nu_o) = 12b$ the error is less than 1%.

2c. Mutual Influences of Atoms

First of all under this heading we have the broadening due to collisions which was first treated by Lorentz.

1. Lorentz Collision Broadening

The physical situation assumed by Lorentz in treating this type of broadening is as follows: an atom absorbs or emits the sharp

frequency ν_0 during the time between two collisions. Each collision stops the radiating or absorption process completely, the energy of vibration being converted completely into kinetic energy. Evidently such a situation gives rise to wave train which is not monochromatic, whence recourse is taken to the expansion of the discontinuous amplitude by means of a Fourier integral to obtain the intensity distribution for a particular time interval between collisions. Then assuming an exponential distribution of this time interval the result for the intensity distribution is shown to be[15)]

$$I_c(\nu) = \frac{\Gamma}{2\pi} \frac{1}{(\nu - \nu_0)^2 + (\Gamma/2)^2} \tag{16}$$

where

$$\Gamma = \frac{1}{\pi\tau} = \varsigma^2 \bar{v} N \tag{17}$$

τ is the mean time between collisions. $\bar{v}$ is the root mean square velocity, N the number of atoms per unit volume. ς is the collision diameter which in reference to experiments on collision broadening is called the "optical collision diameter" in view of the fact that the kinetic theory ς is considerably less than that obtained experimentally in optical experiments. Attempts to obtain ς via classical theories have been futile. Making use of the results (9) and (15) we see that at the wings of the line the distribution of the damping, collision, and Doppler broadening together still yield a dispersion distribution with

$$(\Delta\nu_{1/2})_{C+N} = \gamma_{C+N} = \Gamma + \gamma_N \tag{18}$$

ii. Broadening and Displacement Due to Force Fields of Neighboring Atoms

Two cases are to be distinguished here. On the one hand the atom of interest may be surrounded by foreign atoms and the broadening as a function of the number of foreign atoms per unit volume is commonly known as "pressure broadening". On the other hand the absorbing or emitting gas may be homogeneous; in this case the broadening is known as "resonance broadening" (when the gas in the absorbing column is dilute). "Van der Waal broadening" is a term used in either case when the dilution of the gas in the absorbing column is small so that on the whole the interactions between the atoms follow an inverse 7th power law of force.[9] In the case of resonance broadening the law of force is essentially an inverse 4th power one. The distinction is merely one of convenience in the ensuing calculations of the investigator. For the sake of completeness one should also mention the broadening due to the presence of ions in the absorption or emission tube. In the case of experiments in absorption this type of broadening is unimportant, but it becomes more so in emission.

It would probably take a volume to present the evolution of the quantum theory of the broadening due to the mutual influences of the atoms. Only a brief survey will be given here.

The first attempt at a quantum theory of "Lorentz"[20] broadening was made by Jablonski.[21] He considered a collision between an absorbing atom and a foreign gas molecule (or a similar atom of the same kind) as a

temporary formation of a quasi-molecule. Now by means of quantum mechanics it is possible to compute the perturbation energy of the term values of the atom as a function of the distance apart to obtain the so called Franck-Condon curves. By means of these he was able to give a qualitative explanation of the broadening and shift of spectral lines.

The next important step in the development of an accurate theory was made by Margenau[22] and by Kulp[23]. These investigators extended the ideas of Jablonski, and, by applying the statistical theories of density fluctuations were able to calculate the shift of an absorption line in terms of the pressure of the foreign gas and of the atomic constants. In particular the shift and width were shown to be proportional to the pressure in agreement with experiment.[24]

Weisskopf[25] was the first to develop a somewhat successful theory of "Lorentz" broadening. He showed the quantum mechanical principles involved and provided the mathematical tools for computing the intensity distribution. It was shown that the mathematical manipulations are essentially those of classical theory. According to Weisskopf, "Lorentz" broadening is to be looked upon as a conversion of translational energy into light energy and vice versa according to the old ideas of Minkowski[26] and Oldenberg[27]. From a wave mechanical point of view the process is analogous to the electron-vibration bands of a diatomic molecule in which the energy of motion of the nuclei can be added or subtracted from the electron terms. In the case of the diatomic molecule the spectrum is discrete because of the regular character of the nuclear motion. In the

case of "Lorentz" broadening, however, the two sides of the broadened line represent continuous spectra due to the irregularity of the motions involved. The process then is to be considered as the change of frequency caused by the approach of a perturbing atom so that the phases of the normal vibration before and after collision is no longer in agreement. This idea was first put forward by Lenz.[28] The phase change is obtained as a function of the nuclear position and a so-called distance of closest approach ρ which is determined by setting the phase change equal to unity (Weiskopf). Having ascertained ρ one merely puts it in (17) to obtain Γ. The values of ρ so obtained check as well as is to be expected.[29]

Holztmark[30] was the first to treat the problem of resonance broadening on the basis of the classical theory and this phenomenon is frequently alluded to by his name. He found the broadening to vary as $\sqrt{N}$ f. Shutz and Mensing[31] pointed out that the treatment of Holtzmark when properly carried out should give a line breadth which varies as $\sqrt{N}$f. In no case was the line form computed. However, on the basis of classical dispersion theory Weiskopf[32] obtained an expression for the absorption coefficient of a gas as a function of the frequency. He regarded this type of broadening in the same light as the "Lorentz" broadening. The interaction between the atoms is assumed to be that between two dipoles. In this manner Weiskopf obtains for the half-breadth[33]

(Weiskopf)
$$\Delta\nu_{1/2} \cong \frac{e^2 f_{12}}{2\pi m \nu_0} N \qquad (19)$$

Margeneau[34] on the other hand obtains by his statistical theory

(Margeneau) $$\Delta\nu_{1/2} \simeq \frac{e^2 f_{12}}{6\pi m \nu_0} N \qquad (20)$$

and he points out that the problem of resonance broadening can be dealt with adequately without the use of "collision diameters". (20) differs little from (19).

The next theoretical advance in the treatment of resonance broadening was made by Furssow and Wlassow[35] who treated the problem from the wave mechanical point of view and obtain for the half breadth

(F & W) $$\Delta\nu_{1/2} = \frac{2e^2 f}{3\pi m \nu_0} N \qquad (21)$$

It is seen that (19), (20) and (21) all have the same form but with different numerical factors.

Professor Houston[36] extended the theory to include the fine structure and he showed the approximate equivalence of the various methods in obtaining the spectral line breadths. In particular he obtained

H $$\Delta\nu_{1/2} = \frac{26^{\frac{1}{2}}\ S(J,J')}{h(2J+1)(2J'+1)} N \qquad (22)$$

where S(J,J') is the line strength as defined by Condon and Shortly.[37] (22) shows that $\Delta\nu_{\frac{1}{2}}$ is the same for each member of a Russell-Saunders multiplet. For the alkali resonance lines (22) becomes

$$\Delta\nu_{1/2} = \frac{(6)^{1/2}\ e^2}{8\pi m \nu_0} N \qquad (23)$$

For high pressures or small dilution of the absorbing gas Kuhn[38] maintains that the intensity distribution at the long wave length side follows the law

$$I(\nu) = \frac{\text{const}}{(\nu_0 - \nu)^{3/2}} \qquad (24)$$

thus, under these conditions the line should exhibit an asymmetry. So much then for this necessarily scant review of the theory.

3. Experimental Review

Much work has been done in the field of line broadening especially for the case of broadening by foreign gases.[39] Investigations pertaining to resonance broadening have been somewhat scanty in view of the fact that windows capable of withstanding attack of the absorbing substance have not been long in use. In regard to the verification of natural broadening mention should be made of the outstanding work of Minkowski[40] who considered the resonance lines of sodium and was able to verify the theoretical contours and the half breadths due to radiation damping. Korff[41], Weingeroff[42], and Schutz[43] also obtained somewhat similar results. Perhaps the most important work on natural broadening has been done by Unsold[44] who studied the natural breadth of the H_α line of the solar absorption spectra and was able to verify the correctness of the theoretical contour and the expression peculiar to quantum mechanics for the half breadths as expressed by I(6).

For pressures of the homogeneous absorbing vapor above 10^{-3} mm Hg

various investigators noted an increase in γ with N but disagreement prevailed as to the form of the dependence.[45] More recently however the work of Lloyd,[1] Watanabe[2] and Ch'en[3] seem to yield somewhat consistent results as to the dependence of γ on N. They found a linear dependence. Thus, it seems that the marked improvement in technique brought about by the above investigators is indicative of the correctness of their findings as far as one can ascertain at the present time.

Furthermore, the question as to the ratio of the breadths of a Russell-Saunders multiplet which has been investigated theoretically by Professor Houston[36] and given somewhat careful attention by Lloyd, Watanabe and Ch'en in their work seem s to indicate that for the resonance lines of Na, K[46] and Rb the ratio is not unity as the work of Professor Houston maintains. In fact the ratios seem to vary from element to element in such manner as to show an increase with atomic weight. In particular $\Delta\nu_{1/2}{}^{s}/\Delta\nu_{1/2}{}^{p}$ = 1.16, 1.3,[46] 1.6 for Na, K, and Rb respectively. It is hoped that this theoretical difficulty will be resolved in the near future.

II. General Theory of Line Broadening

In view of the fact that the various theories on line broadening which have appeared in the literature from time to time are lacking in completeness of presentation it was thought desirable to synthesize the various quantum mechanical concepts regarding line broadening into a unified whole. Jablonski[47] as far as this investigation is aware seems to have been the only one to consider the problem in a rather general fashion, but from a different point of view. Here, recourse is taken to Dirac's radiation theory and application of the findings of quantum statistical mechanics[48] is made.

It might be stated, however, that no numerical results have been obtained as yet, although the various matrix elements have been evaluated and will be presented in a later paper - together with the final results if this proves to be feasible. The matrix elements are quite easy to evaluate if one uses the coulomb interaction between the various particles. The model chosen for the atoms is of the hydrogenic type and only the case for homogeneous vapors is worked out although it is not difficult to extend the results to the case when foreign atoms are present.

1. Hamiltonian of System

Consider N hydrogenic atoms in a box. Let R_i denote the radius vector from the origin of the fixed inertial system (box) to the core of the ith atom, R_{ei} the radius vector from O to the electron of interest of the ith atom, r_i the radius vector from the atom core to the electron of

interest. From the figure then:

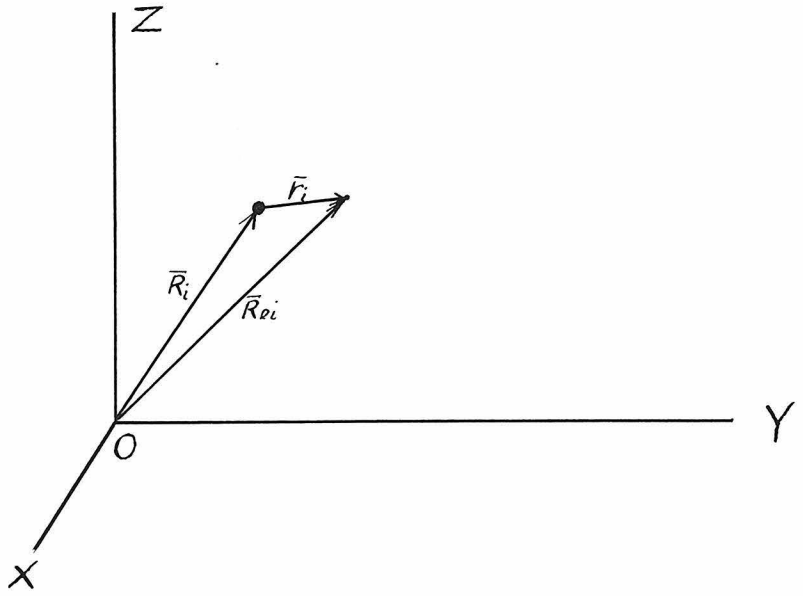

$$R_{ei} = R_i + r_i \tag{1}$$

If M is the mass of the atom core and m the mass of the electron, then the kinetic energy of the ith atom is

$$T_i = \frac{M}{2} \dot{\bar{R}}_i^2 + \frac{m}{2} (\dot{\bar{R}}_i^2 + 2\dot{\bar{r}}_i \dot{\bar{R}}_i + \dot{\bar{r}}_i^2) \tag{2}$$

Now if $V_i(\bar{r}_i)$ is the potential energy of the electron in atom i, and

$$U(\bar{R}_i, \bar{R}_j, \bar{r}_i, \bar{r}_j) \equiv U_{ij} \tag{3}$$

is the interaction between any two atoms, then the Hamiltonian of the system (N atoms) is:

$$H_a = \sum_{i=1}^{N} \left\{ \frac{M}{2}\dot{\bar{R}}_i^2 + \frac{m}{2}(\dot{\bar{R}}_i^2 + 2\dot{\bar{r}}_i\cdot\dot{\bar{R}}_i + \dot{\bar{r}}_i^2) + V_i(\bar{r}_i) + \frac{1}{2}\sum_{j=1}^{N} U_{ij} \right\} \tag{4}$$

In momenta representation (4) becomes $\left(P_i \equiv \frac{\partial L}{\partial \dot{q}_i}\right)$ [49]

$$H_a = \sum_{i=1}^{N} \left\{ \left(\frac{1}{2M} - \frac{m}{M^2}\right)\bar{P}_i^2 + \left(\frac{1}{2m} + \frac{1}{2M}\right)\bar{p}_i^2 - \frac{1}{M}\bar{p}_i\cdot\bar{P}_i + V_i(\bar{r}_i) + \frac{1}{2}\sum_{j=1}^{N} U_{ij} \right\} \tag{5}$$

Now if Radiation is also present, we must add to (5) the radiation Hamiltonian:[50]

$$H_r = \sum_{s} \left\{ \left(\frac{\dot{q}_s^2}{2} + \frac{\omega_s^2 q_s^2}{2}\right) - \frac{e}{m}\sum_{i=1}^{N} c\sqrt{\frac{2}{\Omega}}\,\bar{a}_s q_s \cdot \sin\frac{\omega_s}{c}[\bar{\alpha}_s\cdot(\bar{R}_i+\bar{r}_i)+\beta_s]\;\bar{P}_i \right\} \tag{6}$$

where the interaction of radiation with the core is left out; when it is included we must add to (6) (if it is assumed that the non-valence electrons neutralize the protons and the atom core is essentially point-like)

$$\sum_{s}\frac{e}{M}\sum_{i=1}^{N} c\sqrt{\frac{2}{\Omega}}\,\bar{a}_s q_s \sin\frac{\omega_s}{c}[\bar{\alpha}_s\cdot\bar{R}_i+\beta_s]\cdot(\bar{P}_i - \bar{P}_i) \tag{7}$$

Also terms in A^2 are left out. (Neglect of two quantum processes.)

The total Hamiltonian of the system is then given by adding (5), (6) and perhaps (7). Doing so we may write:

$$H = H_0 + H_1 + H_2, \tag{8}$$

where

$$H_0 = \sum_{i=1}^{N} \left(\frac{1}{2M} - \frac{m}{M^2}\right)\bar{P}_i^2 + \left(\frac{1}{2M} + \frac{1}{2m}\right)\bar{p}_i^2 + V_i(\bar{r}_i) + \sum_s \left(\frac{\dot{q}_s^2}{2} + \frac{\omega_s^2 q_s^2}{2}\right)$$

$$H_1 = \frac{1}{2} \sum_{i \neq j} U_{ij}(\bar{R}_i, \bar{R}_j, \bar{r}_i, \bar{r}_j) \tag{9}$$

$$H_2 = \sum_{i=1}^{N} \left\{ -\frac{\bar{p}_i \cdot \bar{P}_i}{M} - \frac{e}{m} \sum_s c\sqrt{\frac{2}{\Omega}}\, a_s q_s \sin \frac{\omega_s}{c}\left[\bar{\alpha}_s \cdot (\bar{R}_i + \bar{r}_i) + \beta_s\right] \cdot \bar{p}_i \right\}$$

2. Zero Order Wave Functions

There are various possibilities as to the kinds of wave functions that one uses in obtaining the matrix elements. In the first place, for the sake of simplicity, and in the second place, since one is usually interested in the case when the dilution of atoms in the box is large, we shall choose wave functions which can be factored into one part containing the external coordinates, one the internal coordinates, and still another part containing the radiation variables.

Let $\psi_{\varepsilon_i}(\bar{r}_i)$ be a solution of

$$\left[\left(\frac{1}{2M}+\frac{1}{2m}\right)\bar{P}_i^2+V_i(\bar{r}_i)\right]\psi_{\varepsilon_i}(\bar{r}_i)=\varepsilon_i\,\psi_{\varepsilon_i}(\bar{r}_i) \tag{1}$$

Also let $\psi_{E_i}(\bar{R}_i)$ be a solution of

$$\left(\frac{1}{2M}-\frac{m}{M^2}\right)\bar{P}_i^2\psi_{E_i}(\bar{R}_i)=E_i\,\psi_{E_i}(\bar{R}_i), \tag{2}$$

and finally let $\Phi_{n_s}(q_s)$ be a solution of

$$\frac{1}{2}\left(\dot{q}_s^2+\omega_s^2 q_s^2\right)\Phi_{n_s}(q_s)=\hbar\omega_s\left(n_s+\tfrac{1}{2}\right)\Phi_{n_s}(q_s) \tag{3}$$

The above equation determines the radiation wave functions according to the Dirac quantization of the radiation field.[50] If (1), (2), and (3) hold, then

$$\Psi_{E_T}=\prod_{i=1}^{N}\psi_{\varepsilon_i}(\bar{r}_i)\,\psi_{E_i}(\bar{R}_i)\prod_{s}\Phi_{n_s}(q_s) \tag{4}$$

is a solution of

$$H_0\,\Psi_{E_T}=E_T\,\Psi_{E_T} \tag{5}$$

where H_0 is given by 1-(9), and

$$E_T=\sum_{i=1}^{N}(\varepsilon_i+E_i)+\sum_{s}\hbar\omega_s\left(n_s+\tfrac{1}{2}\right) \tag{6}$$

Furthermore, it is still possible to build up a more general solution than that given by (4) by multiplying it by suitable constants and summing over the permutations of the particle indices.[51] At the present moment, however, there seems to be some difference of opinion as

to the choice in view of the fact that our internal coordinates are relative ones so that it is not obvious, off hand, as to what combinations should be chosen so as to satisfy Pauli's principal for the electrons of interest. Nevertheless, what is to follow does not make use of this point.

3. General Solution of Un-Perturbed System. Solution when H_1 and H_2 included.

a. Equations for C's.

When the perturbations given in 1-(9) are neglected altogether, namely H_1 and H_2, the general solution of 2-(5) when written in time dependent form is

$$\Psi(t) = \sum_{E_T} C(E_T)\, \psi_{E_T}\, e^{-\frac{E_T t_i}{\hbar}} \tag{1}$$

where the C's are constants.

In case the perturbations H_1 and H_2 are included, then the general solution may be expressed as:

$$\Psi(t) = \sum_{E_T} C_{E_T}(t)\, \psi_{E_T}\, e^{-\frac{E_T t_i}{\hbar}} \tag{2}$$

where now the C's are functions of the time. If (2) is put in

$$-\frac{\hbar}{i}\frac{\partial \Psi}{\partial t} = (H_0 + H_1 + H_2)\,\Psi \tag{3}$$

then by the method of variation of constants the C's must satisfy the equations[50]

$$i\hbar \dot{C}_{E_T} = \sum_{E'_T} (E_T | H_1 + H_2 | E'_T) C_{E'_T} e^{i\frac{E_T - E'_T}{\hbar}t} . \qquad (4)$$

b. Examination of 3-a-(4)

Now from 1-(9) one sees that H_1 does not contain q_s, hence $(E_T | H_1 | E'_T)$ will be nil unless the state of the radiation field is unaltered. H_2 contains $\bar{p}_i \cdot \bar{P}_i$ and q_s. But since the average momentum $\bar{\bar{P}}_i = 0$ we may disregard this term in H_2. The fact that q_s occurs requires that the energy of the radiation field change in such manner that it suffers an increase or decrease of one quantum, say, $\hbar\omega_s$. Utilizing these facts (4) may be written as

$$i\hbar C\begin{pmatrix} \breve{E}_T \\ n \end{pmatrix} = \sum_{\breve{E}'_T} \begin{pmatrix} \breve{E}_T \\ n \end{pmatrix} H_1 \begin{pmatrix} \breve{E}'_T \\ n \end{pmatrix} C\begin{pmatrix} \breve{E}'_T \\ n \end{pmatrix} e^{i\frac{\breve{E}_T - \breve{E}'_T}{\hbar}t}$$

$$+ \sum_{\breve{E}'_T, s} \begin{pmatrix} \breve{E}_T \\ n \end{pmatrix} H_2 \begin{pmatrix} \breve{E}'_T \\ n+1_s \end{pmatrix} C\begin{pmatrix} \breve{E}'_T \\ n+1_s \end{pmatrix} e^{i\frac{\breve{E}_T - \breve{E}'_T - \hbar\omega_s}{\hbar}t}$$

$$+ \sum_{\breve{E}'_T, s} \begin{pmatrix} \breve{E}_T \\ n \end{pmatrix} H_2 \begin{pmatrix} \breve{E}'_T \\ n-1_s \end{pmatrix} C\begin{pmatrix} \breve{E}'_T \\ n-1_s \end{pmatrix} e^{i\frac{\breve{E}_T - \breve{E}'_T + \hbar\omega_s}{\hbar}t} \qquad (5)$$

where $\breve{E}_T$ denotes the total atomic (el. + core) energy, and n denotes the initial state of the radiation field. $* \; l_s$ denotes that one quantum $\hbar\omega_s$ has been emitted or absorbed.

3c. Approximate Solution of 3-b-(5)

Assume that initially

$$C\begin{pmatrix}\breve{E}_T \\ n\end{pmatrix} = C\begin{pmatrix}\breve{E}_T \\ n \pm l_s\end{pmatrix} = 0 \; ; \quad C\begin{pmatrix}\breve{E}'_T \\ n\end{pmatrix} = e^{-\gamma t} \tag{6}$$

Putting (6) in (5) we obtain

$$\hbar i \dot{C}\begin{pmatrix}\breve{E}_T \\ n\end{pmatrix} = \left(\begin{matrix}\breve{E}_T \\ n\end{matrix} \middle| H_1 \middle| \begin{matrix}\breve{E}'_T \\ n\end{matrix}\right) e^{i\frac{\breve{E}_T - \breve{E}'_T}{\hbar}t - \gamma t} \tag{7}$$

(5) also gives with (6) substituted

$$\hbar i \dot{C}\begin{pmatrix}\breve{E}_T \\ n+l_s\end{pmatrix} = \left(\begin{matrix}\breve{E}_T \\ n+l_s\end{matrix} \middle| H_2 \middle| \begin{matrix}\breve{E}'_T \\ n\end{matrix}\right) e^{i\frac{\breve{E}_T - \breve{E}'_T + \hbar\omega_s}{\hbar}i - \gamma t} \tag{8}$$

and also

$$\hbar i \dot{C}\begin{pmatrix}\breve{E}_T \\ n-l_s\end{pmatrix} = \left(\begin{matrix}\breve{E}_T \\ n-l_s\end{matrix} \middle| H_2 \middle| \begin{matrix}\breve{E}'_T \\ n\end{matrix}\right) e^{i\frac{\breve{E}_T - \breve{E}'_T - \hbar\omega_s}{\hbar}t - \gamma t} \tag{9}$$

And finally (5) gives

$$\hbar i \dot{C}\begin{pmatrix} \breve{E}_T' \\ n \end{pmatrix} = \sum_{\breve{E}_T} \left(\begin{matrix} \breve{E}_T' \\ n \end{matrix} \middle| H_1 \middle| \begin{matrix} \breve{E}_T \\ n \end{matrix} \right) C\begin{pmatrix} \breve{E}_T \\ n \end{pmatrix} e^{i\frac{\breve{E}_T' - \breve{E}_T}{\hbar}t}$$

$$+ \sum_{E_T, S} \left(\begin{matrix} \breve{E}_T' \\ n \end{matrix} \middle| H_2 \middle| \begin{matrix} \breve{E}_T \\ n+1_S \end{matrix} \right) C\begin{pmatrix} \breve{E}_T \\ n+1_S \end{pmatrix} e^{i\frac{\breve{E}_T' - \breve{E}_T - \hbar\omega_S}{\hbar}t}$$

$$+ \sum_{E_T, S} \left(\begin{matrix} \breve{E}_T' \\ n \end{matrix} \middle| H_2 \middle| \begin{matrix} \breve{E}_T \\ n-1_S \end{matrix} \right) C\begin{pmatrix} \breve{E}_T \\ n-1_S \end{pmatrix} e^{i\frac{\breve{E}_T' - \breve{E}_T + \hbar\omega_S}{\hbar}t} \qquad (10)$$

The solutions of (7), (8), and (9) which satisfy the conditions (6) at t = 0 are

$$C\begin{pmatrix} \breve{E}_T \\ n \end{pmatrix} = \left(\begin{matrix} \breve{E}_T \\ n \end{matrix} \middle| H_1 \middle| \begin{matrix} \breve{E}_T' \\ n \end{matrix} \right) \frac{1 - e^{i\frac{(\breve{E}_T - \breve{E}_T')t}{\hbar} - \gamma t}}{\hbar\left[\frac{\breve{E}_T - \breve{E}_T'}{\hbar} + i\gamma\right]} \qquad (11)$$

$$C\begin{pmatrix} \breve{E}_T \\ n+1_S \end{pmatrix} = \left(\begin{matrix} \breve{E}_T \\ n+1_S \end{matrix} \middle| H_2 \middle| \begin{matrix} \breve{E}_T' \\ n \end{matrix} \right) \frac{1 - e^{i\frac{(\breve{E}_T - \breve{E}_T' + \hbar\omega_S)t - \gamma t}{\hbar}}}{\hbar\left[\frac{\breve{E}_T - \breve{E}_T' + \hbar\omega_S}{\hbar} + i\gamma\right]} \qquad (12)$$

$$C\begin{pmatrix} \breve{E}_T \\ n-1_S \end{pmatrix} = \left(\begin{matrix} \breve{E}_T \\ n-1_S \end{matrix} \middle| H_2 \middle| \begin{matrix} \breve{E}_T' \\ n \end{matrix} \right) \frac{1 - e^{i\frac{(\breve{E}_T - \breve{E}_T' - \hbar\omega_S)t - \gamma t}{\hbar}}}{\hbar\left[\frac{\breve{E}_T - \breve{E}_T' - \hbar\omega_S}{\hbar} + i\gamma\right]} \qquad (13)$$

But (11), (12), (13) must satisfy (10), hence putting on the left of (10), $C\binom{E'_T}{n} = e^{-\gamma t}$ and on the right (11), (12) and (13), (10) gives

$$-\hbar i\gamma e^{-\gamma t} = \sum_{E_T} \left(\begin{matrix} E'_T \\ n \end{matrix}\middle| H_1 \middle| \begin{matrix} E_T \\ n \end{matrix}\right)\left(\begin{matrix} E_T \\ n \end{matrix}\middle| H_1 \middle| \begin{matrix} E'_T \\ n \end{matrix}\right) \times \frac{e^{i\frac{E'_T - E_T}{\hbar}t} - e^{-\gamma t}}{\hbar\left[\frac{E_T - E'_T}{\hbar} + i\gamma\right]}$$

$$+ \sum_{E_T, s} \left(\begin{matrix} E'_T \\ n \end{matrix}\middle| H_2 \middle| \begin{matrix} E_T \\ n+1_s \end{matrix}\right)\left(\begin{matrix} E_T \\ n+1_s \end{matrix}\middle| H_2 \middle| \begin{matrix} E'_T \\ n \end{matrix}\right) \times \frac{e^{i\frac{E'_T - E_T - \hbar\omega_s}{\hbar}t} - e^{-\gamma t}}{\hbar\left[\frac{E_T - E'_T + \hbar\omega_s}{\hbar} + i\gamma\right]}$$

$$+ \sum_{E_T, s} \left(\begin{matrix} E'_T \\ n \end{matrix}\middle| H_2 \middle| \begin{matrix} E_T \\ n-1_s \end{matrix}\right)\left(\begin{matrix} E_T \\ n-1_s \end{matrix}\middle| H_2 \middle| \begin{matrix} E'_T \\ n \end{matrix}\right) \times \frac{e^{i\frac{E'_T - E_T + \hbar\omega_s}{\hbar}t} - e^{-\gamma t}}{\hbar\left[\frac{E_T - E'_T - \hbar\omega_s}{\hbar} + i\gamma\right]} \qquad (14)$$

Or rewriting (14) we obtain

$$\hbar i\gamma = \sum_{\tilde{E}_T} \left(\begin{matrix}\tilde{E}_T' \\ n\end{matrix}\middle| H_1 \middle| \begin{matrix}\tilde{E}_T \\ n\end{matrix}\right)\left(\begin{matrix}\tilde{E}_T \\ n\end{matrix}\middle| H_1 \middle| \begin{matrix}\tilde{E}_T' \\ n\end{matrix}\right) \frac{1-e^{\left[i\,\frac{\tilde{E}_T'-\tilde{E}_T}{\hbar}+\gamma\right]t}}{\hbar\left[\frac{\tilde{E}_T-\tilde{E}_T'}{\hbar}+i\gamma\right]} +$$

$$\sum_{\tilde{E}_T,\,s} \left(\begin{matrix}\tilde{E}_T' \\ n\end{matrix}\middle| H_2 \middle| \begin{matrix}\tilde{E}_T \\ n+1_s\end{matrix}\right)\left(\begin{matrix}\tilde{E}_T \\ n+1_s\end{matrix}\middle| H_2 \middle| \begin{matrix}\tilde{E}_T' \\ n\end{matrix}\right) \frac{1-e^{\left[i\,\frac{\tilde{E}_T'-\tilde{E}_T-\hbar\omega_s}{\hbar}+\gamma\right]t}}{\hbar\left[\frac{\tilde{E}_T-\tilde{E}_T'+\hbar\omega_s}{\hbar}+i\gamma\right]} +$$

$$\sum_{\tilde{E}_T,\,s} \left(\begin{matrix}\tilde{E}_T' \\ n\end{matrix}\middle| H_2 \middle| \begin{matrix}\tilde{E}_T \\ n-1_s\end{matrix}\right)\left(\begin{matrix}\tilde{E}_T \\ n-1_s\end{matrix}\middle| H_2 \middle| \begin{matrix}\tilde{E}_T' \\ n\end{matrix}\right) \frac{1-e^{\left[i\,\frac{\tilde{E}_T'-\tilde{E}_T+\hbar\omega_s}{\hbar}+\gamma\right]t}}{\hbar\left[\frac{\tilde{E}_T-\tilde{E}_T'-\hbar\omega_s}{\hbar}+i\gamma\right]} \qquad (15)$$

3d. Evaluation of γ in 3-c-(15)

Now in (15) H_1 does not contain q_s hence the matrix elements of H_1 in (15) may be written simply as:

$$(\tilde{E}_T' |\ H_1 |\ \tilde{E}_T) \qquad (16)$$

Now H_2 on the other hand contains q_s as a factor. Whence if we define

$$H_2 = \sum_{i=1,\,s}^{N} g_s\, H_{si} \qquad (17)$$

where H_{gi} depends only on the external and internal coordinates, the

contribution of the radiation field to the ($|H_z|$) may be readily ascertained. Now

$$\left(\begin{matrix}\tilde{E}_T' \\ n\end{matrix}\middle|H_z\middle|\begin{matrix}\tilde{E}_T \\ n+1_s\end{matrix}\right) = \sum_{i=1}^{N}\left(\tilde{E}_T'|H_{si}|\tilde{E}_T\right)\left(n|g_s|n+1_s\right)$$

and $$\left(\begin{matrix}\tilde{E}_T' \\ n\end{matrix}\middle|H_z\middle|\begin{matrix}\tilde{E}_T \\ n-1_s\end{matrix}\right) = \sum_{i=1}^{N}\left(\tilde{E}_T'|H_{si}|\tilde{E}_T\right)\left(n|g_s|n-1_s\right) \qquad (18)$$

Comparing (17) with 1 - (9) we see that

$$H_{si} = -\frac{ec}{m}\sqrt{\frac{2}{\Omega}}\,\bar{a}_s \sin\frac{\omega_s}{c}\left[\bar{\alpha}_s\cdot(\bar{R}_i+\bar{r}_i)+\beta_s\right]\cdot\bar{p}_i \qquad (19)$$

Hence if we define

$$H_s \equiv \sum_i H_{si} \qquad (20)$$

(18) becomes

$$\left(\begin{matrix}\tilde{E}_T' \\ n\end{matrix}\middle|H_z\middle|\begin{matrix}\tilde{E}_T \\ n+1_s\end{matrix}\right) = \left(\tilde{E}_T'|H_s|\tilde{E}_T\right)\left(n|g_s|n+1_s\right)$$

$$\left(\begin{matrix}\tilde{E}_T' \\ n\end{matrix}\middle|H_z\middle|\begin{matrix}\tilde{E}_T \\ n-1_s\end{matrix}\right) = \left(\tilde{E}_T'|H_s|\tilde{E}_T\right)\left(n|g_s|n-1_s\right) \qquad (21)$$

But $$\left(n|g_s|n+1_s\right) = \left[\frac{\hbar(n_s+1)}{2\omega_s}\right]^{\frac{1}{2}}$$

$$\left(n|g_s|n-1_s\right) = \left[\frac{\hbar n_s}{2\omega_s}\right]^{\frac{1}{2}} \qquad (22)$$

Hence if we put (16), (21), and (22) in (15) it becomes if we define:

$$(\tilde{E}'_\tau|H_1|\tilde{E}_\tau)(\tilde{E}_\tau|H_1|\tilde{E}'_\tau) \equiv A(\tilde{E}'_\tau, \tilde{E}_\tau)$$

$$(\tilde{E}'_\tau|H_s|\tilde{E}_\tau)(\tilde{E}_\tau|H_s|\tilde{E}'_\tau) \equiv B(\omega_s, \tilde{E}'_\tau, \tilde{E}_\tau) \,, \tag{23}$$

$$\hbar i\gamma = \sum_{\tilde{E}_\tau} A(\tilde{E}'_\tau, \tilde{E}_\tau) \frac{1 - e^{\left[i\frac{\tilde{E}'_\tau - \tilde{E}_\tau}{\hbar} + \gamma\right]t}}{\hbar\left[\frac{\tilde{E}_\tau - \tilde{E}'_\tau}{\hbar} + i\gamma\right]} +$$

$$\sum_{\tilde{E}_\tau, s} \frac{\hbar(n_s+1)}{2\omega_s} B(\omega_s, \tilde{E}'_\tau, \tilde{E}_\tau) \frac{1 - e^{\left[i\frac{\tilde{E}'_\tau - \tilde{E}_\tau - \hbar\omega_s}{\hbar} + \gamma\right]t}}{\hbar\left[\frac{\tilde{E}_\tau - \tilde{E}'_\tau + \hbar\omega_s}{\hbar} + i\gamma\right]} +$$

$$\sum_{\tilde{E}_\tau, s} \frac{\hbar n_s B(\omega_s, \tilde{E}'_\tau, \tilde{E}_\tau)}{2\omega_s} \frac{1 - e^{\left[i\frac{\tilde{E}'_\tau - \tilde{E}_\tau + \hbar\omega_s}{\hbar} + \gamma\right]t}}{\hbar\left[\frac{\tilde{E}_\tau - \tilde{E}'_\tau - \hbar\omega_s}{\hbar} + i\gamma\right]} \tag{24}$$

Now in (24) we may replace the summation over s by an integration after multiplying by

$$dn = \frac{\Omega}{2\pi^3 C^3}\omega_s^2 d\omega_s, \tag{25}$$

doing so and applying the theorem:

$$\int f(\nu)\frac{1-e^{[i(\nu-\nu_0)+\gamma]t}}{\nu_0-\nu+i\gamma}\,d\nu = \pi i f(\nu_0), \tag{26}$$

(24) becomes

$$\hbar i\gamma =$$

$$\sum_{\breve{E}_T} A(\breve{E}_T', \breve{E}_T)\frac{1-e^{[i\frac{\breve{E}_T'-\breve{E}_T}{\hbar}+\gamma]t}}{\hbar\left[\frac{\breve{E}_T-\breve{E}_T'}{\hbar}+i\gamma\right]}$$

$$\frac{i\Omega}{4\pi^2 C^3}\sum_{\breve{E}_T}\int\left[n\left(\left|\frac{\breve{E}_T'-\widetilde{E}_T}{\hbar}\right|\right)+1\right]\left|\widetilde{E}_T'-\widetilde{E}_T\right| B\left(\frac{\breve{E}_T'-\widetilde{E}_T}{\hbar}, \widetilde{E}_T', \widetilde{E}_T\right)d\widetilde{\Omega}$$

$$\frac{i\Omega}{4\pi^2 C^3}\sum_{\widetilde{E}_T}\int n\left(\left|\frac{\widetilde{E}_T'-\widetilde{E}_T}{\hbar}\right|\right)\left|\widetilde{E}_T'-\widetilde{E}_T\right| B\left(\frac{\widetilde{E}_T'-\widetilde{E}_T}{\hbar}, \widetilde{E}_T', \widetilde{E}_T\right)d\widetilde{\Omega} \tag{27}$$

where $n\left(\left|\frac{\breve{E}_T'-\widetilde{E}_T}{\hbar}\right|\right)$ is the number of light quanta whose energy is

$$(|\breve{E}'_T - \breve{E}_T|) \tag{28}$$

$\int d\breve{\Omega}$ represents summation over all directions of propagation and summation over both directions of polarization. The last two terms in (27) contribute to the so-called radiation damping and is inappreciable when the number of atoms in the box is large, that is in comparison with the first term in (27). Hence we shall exclude these two terms and concentrate on the first term of (27). In the approximation, (27) gives:

$$\hbar i\gamma \cong \sum_{\breve{E}_T} A(\breve{E}'_T - \breve{E}_T)\, \frac{1 - e^{\left[i\frac{\breve{E}'_T - \breve{E}_T}{\hbar} + \gamma\right]t}}{\hbar\left[\frac{\breve{E}_T - \breve{E}'_T}{\hbar} + i\gamma\right]} \tag{29}$$

Now $\sum_{\breve{E}_T}$ means $\sum_{\mathcal{E},E}$, where $\mathcal{E}$ denotes the total internal state and $\breve{E}$ the total external state, hence (29) gives

$$\hbar i\gamma \cong \sum_{\mathcal{E},E} A(\breve{E}'_T, \mathcal{E}+E)\, \frac{1 - e^{\left[i\frac{\breve{E}'_T - \mathcal{E} - E}{\hbar} + \gamma\right]t}}{\hbar\left[\frac{\mathcal{E}+E-\breve{E}'_T}{\hbar} + i\gamma\right]} \tag{30}$$

Now if the box is large the external energy states will be very dense, whence we may replace the summation over E by an integration after multiplying by

$$G(E)\,dE \tag{31}$$

where G(E) is the number of external energy states between E and E + dE. Doing so and applying (26), (30) becomes

$$\hbar i \gamma \cong \pi i \sum_{\varepsilon} G(\tilde{E}'_T - \varepsilon)\, A(\tilde{E}'_T, \tilde{E}'_T) \tag{32}$$

or

$$\gamma \cong \frac{\pi}{\hbar} \sum_{\varepsilon} G(\tilde{E}'_T - \varepsilon)\, A(\tilde{E}'_T, \tilde{E}'_T) \tag{33}$$

which is dimensionally correct since $[A(\tilde{E}'_T, \tilde{E}'_T)] = [E^2]$, and $[G(\tilde{E}'_T - \varepsilon)] = [E^{-1}]$. In (33)

$$A(\tilde{E}'_T, \tilde{E}'_T) = \left(\begin{matrix} E' \\ \varepsilon' \end{matrix} \middle| H_1 \middle| \begin{matrix} E'-\varepsilon \\ \varepsilon \end{matrix} \right) \left(\begin{matrix} E'-\varepsilon \\ \varepsilon \end{matrix} \middle| H_1 \middle| \begin{matrix} E' \\ \varepsilon' \end{matrix} \right) \tag{34}$$

Putting (34) in (33) we finally have

$$\gamma \cong \frac{\pi}{\hbar} \sum_{\varepsilon} G(E'+\varepsilon'-\varepsilon) \left| \left(\begin{matrix} E' \\ \varepsilon' \end{matrix} \middle| H_1 \middle| \begin{matrix} E'-\varepsilon \\ \varepsilon \end{matrix} \right) \right|^2 \tag{35}$$

4. Case for Absorption

From 3-c-(13) we have

$$C\begin{pmatrix}\tilde{E}_T\\ n-1_S\end{pmatrix}=\begin{pmatrix}\tilde{E}_T\\ n-1_S\end{pmatrix}H_2\Big|\begin{matrix}\tilde{E}_T'\\ n\end{pmatrix}\frac{1-e^{\left[i\frac{\tilde{E}_T-\tilde{E}_T'-\hbar\omega_S}{\hbar}-\gamma\right]t}}{\hbar\left[\frac{\tilde{E}_T-\tilde{E}_T'-\hbar\omega_S}{\hbar}+i\gamma\right]} \tag{1}$$

Now (1) may be written as

$$C\begin{pmatrix}\tilde{E}_T\\ n-1_S\end{pmatrix}=\sum_{\tilde{E}_T''}\begin{pmatrix}\tilde{E}_T\\ n-1_S\end{pmatrix}H_2\Big|\begin{matrix}\tilde{E}_T''\\ n\end{pmatrix}\frac{1-e^{\left[i\frac{\tilde{E}_T-\tilde{E}_T''-\hbar\omega_S}{\hbar}-\gamma\right]t}}{\hbar\left[\frac{\tilde{E}_T-\tilde{E}_T''-\hbar\omega_S}{\hbar}+i\gamma\right]}C_{\tilde{E}_T''}(0) \tag{2}$$

where $C_{\tilde{E}_T''}(0)=0$ unless $\tilde{E}_T''=\tilde{E}_T'$. Similarly if we write the complex conjugate of (2) and multiply we obtain

$$\left|C\begin{pmatrix}\tilde{E}_T\\ n-1_S\end{pmatrix}\right|^2=\frac{1}{\hbar^2}\sum_{\tilde{E}_T'',\tilde{E}_T'''}\begin{pmatrix}\tilde{E}_T\\ n-1_S\end{pmatrix}H_2\Big|\begin{matrix}\tilde{E}_T''\\ n\end{pmatrix}\begin{pmatrix}\tilde{E}_T\\ n-1_S\end{pmatrix}H_2\Big|\begin{matrix}\tilde{E}_T'''\\ n\end{pmatrix}\times$$

$$\frac{1-e^{\left[i\frac{\tilde{E}_T-\tilde{E}_T''-\hbar\omega_S}{\hbar}t-\gamma t\right]}}{\frac{\tilde{E}_T-\tilde{E}_T''-\hbar\omega_S}{\hbar}+i\gamma}\times\frac{1-e^{\left[-i\frac{\tilde{E}_T-\tilde{E}_T'''-\hbar\omega_S}{\hbar}t-\gamma t\right]}}{\frac{\tilde{E}_T-\tilde{E}_T'''-\hbar\omega_S}{\hbar}-i\gamma}\times C_{\tilde{E}_T''}(0)C^*_{\tilde{E}_T'''}(0). \tag{3}$$

But from the postulate of equal a priori probabilities and random phases of statistical mechanics[52)]

$$\overline{C_{\tilde{E}_T''}(0)C^*_{\tilde{E}_T'''}(0)}=\frac{1}{G_{\tilde{E}_T''}}\delta_{\tilde{E}_T''\tilde{E}_T'''} \tag{4}$$

where $G_{\tilde{E}_T}$ is the total number of precise states corresponding to the initial conditions. If we put t large in (3) and also (4), it becomes:

$$\left|C\left(\begin{matrix}\tilde{E}_T \\ n\text{-}1_S\end{matrix}\right)^{\infty}\right|^2 = \frac{1}{\hbar^2 G_{\tilde{E}_T}} \sum_{\tilde{E}'_T} \frac{\left|\left(\begin{matrix}\tilde{E}_T \\ n\text{-}1_S\end{matrix}\middle| H_2 \middle| \begin{matrix}\tilde{E}'_T \\ n\end{matrix}\right)\right|^2}{\left[\frac{\tilde{E}_T - \tilde{E}'_T + \hbar\omega_S}{\hbar}\right]^2 + \gamma^2(E', \mathcal{E}', \mathcal{E})} \tag{5}$$

which is the probability that the system will be found in the state indicated. Now the final state $\left(\begin{matrix}\tilde{E}_T \\ n\text{-}1_S\end{matrix}\right)$ consists of E and $\mathcal{E}$. Furthermore the state of interest is the internal one corresponding to $\mathcal{E}$. Hence if we sum (5) over all external states E we will obtain the probability that the system is finally in some internal state $\mathcal{E}$. Doing so we obtain

$$\left|C\left(\begin{matrix}\mathcal{E} \\ n\text{-}1_S\end{matrix}\right)^{\infty}\right|^2 = \frac{1}{\hbar^2 G_{\tilde{E}_T}} \sum_{E, E', \mathcal{E}'} \frac{\left|\left(\begin{matrix}\tilde{E}_T \\ n\text{-}1_S\end{matrix}\middle| H_2 \middle| \begin{matrix}\tilde{E}'_T \\ n\end{matrix}\right)\right|^2}{\left[\frac{\tilde{E}_T - \tilde{E}'_T + \hbar\omega_S}{\hbar}\right]^2 + \gamma^2(E', \mathcal{E}', \mathcal{E})} \tag{6}$$

Now the external energy states are very dense so the summations in (6) over E and E' may be represented by a double integral after multiplying by

$$G(E)D(E')dEdE' \tag{7}$$

where G(E)dE is the number of states between E and E + dE. (7) becomes then:

$$\left|C\begin{pmatrix}\mathcal{E}\\ n\text{-}1_S\end{pmatrix}^{\infty}\right|^2 = \frac{1}{G_{\tilde{E}'_T}\hbar^2}\sum_{\mathcal{E}'}\int_0^{\infty}\int \frac{G(E)G(E')\left|\begin{pmatrix}E\\ \mathcal{E}\\ n\text{-}1_S\end{pmatrix}H_2\begin{pmatrix}E'\\ \mathcal{E}'\\ n\end{pmatrix}\right|^2}{\left(\frac{E+\mathcal{E}-E'-\mathcal{E}'+\hbar\omega_S}{\hbar}\right)^2+\gamma^2(E',\mathcal{E}',\mathcal{E})}\,dE\,dE' \qquad (8)$$

Now if we assume that initially all of the atoms are in the ground state internally, then the number of precise internal states is 1. On the other hand, if G(E) is the number of states between E and E + dE then

$$G_{E'} = \int G(E)\,dE \qquad (9)$$

is the total number of precise external states. Hence the total number of precise states corresponding to the initial conditions is

$$G_{\tilde{E}'_T} = 1 \times \int G(E)\,dE \qquad (10)$$

And for this case we need not sum over $\mathcal{E}$ in (8) but merely put $\mathcal{E}' = \mathcal{E}^0$, the internal ground state energy of all the atoms.

The result given in (8) is related proportional to the intensity distribution. It remains, however, to evaluate the expressions therein. But this will be postponed for the time being, although, as mentioned in the beginning the matrix elements are not difficult to evaluate. There seems to be some difficulty as to the proper combinations of the zero order wave functions described in 2.

III. The Method and Apparatus

The apparatus and procedure employed in the present work is essentially that first employed by P. E. Lloyd[1] and later by K. Watanabe[2] and Shang-yi Ch'en[3]. In Lloyd's thesis an ample description of the apparatus and method employed is given, hence it would be rather superfluous to give a detailed description here. Nevertheless, a brief summary of the method and apparatus will be given where improvements in technique and measurements will be especially emphasized.

1. Source

The high intensity lamp consists of a replaceable tungsten filament which is 40 mils in diameter and about 3 cms long. The filament is supported rigidly by two nickel electrodes, which have recently been replaced by a pair of new ones. The lamp is operated in vacuo at various amperages depending on the circumstances. It was found that the lifetime of the filament is about 26 hours when operated at 70 amps and drops down to about three or four hours when operated at about 80 amps. In the study of the resonance lines in run #1 the lamp was operated at 70 amps, thus requiring about 26 hours with slit from 20 μ to 50 μ wide. In run #2 the lamp was run at about 80 - 85 amps with the slit from 20 μ to 50 μ wide and required about three or four filament changes to get the required exposure.

At 70 amps the temperature of the filament is approximately 3200°K and at 80 - 85 amps approximately 3400°K. Consequently, because of heat

conduction, it was necessary to cool the electrodes to prevent the wax joints of the lamp from melting. Previously the method of air cooling was used, but it was found that the electrodes could be adequately cooled by using water. This was done in the following manner. Copper tubing was wound and soldered on to the electrodes. Water was diverted from the mercury diffusion pump system and allowed to circulate through the copper tubing, in this manner cooling the leads. This device, it was found, is much more effective than air cooling. In fact it was possible to touch the electrodes while the lamp was operating without ill-effects. This was not possible when air cooling was used. In this manner also much noise was avoided.

The length of the image of the filament on the slit was approximately 2.5 cm and the central portion of about 1 cm was used so that the intensity across the slit was rather uniform as subsequent measurements showed. Uniformity of intensity is important since the astigmatism method (to be dealt with later) of studying the line contour holds only in this case. (It being assumed, of course, that, a priori, in other cases we do not know the intensity function across the slit.)

The intensity of the source in the wave length region of the first member of the principle series of Cs is approximately a maximum. In the immediate region of the doublets then the intensity of the source could be considered as approximately constant. This fact is rather difficult to justify experimentally inasmuch as the variation of sensitivity of the I - P plates used is considerable, especially so in the case of the region

of the $^2P_{3/2}$ component.

2. Furnace and Absorption Cell

Lloyd[1] and Hughes designed and constructed the furnace that was used. It consists briefly of a porcelain cylinder which was wound externally with molybdenum wire in such a manner that the central portion had less windings than the other ends. This cylinder (porcelain) is in turn enclosed within a steel jacket made up of two concentric cylindrical shells in between which water is allowed to circulate. The furnace could be made vacuum tight by means of two steel caps and rubber gaskets of appropriate size. These steel caps are provided with ordinary glass windows. In order to aid in keeping the temperature constant within the furnace the inside part of the water jacket is chromium-plated and well polished. The measurement of the temperature within the absorption cell is made possible by means of a suitable inlet for the thermocouple. Similarly inlets for the electrodes and outlets to the vacuum pumping system were provided. Here previously as in the case of the tungsten lamp the electrodes were air-cooled. It was found that the electrodes could be properly water-cooled by winding copper tubing into helical form so as to enclose the electrodes.

Originally too it was found that the insertion and removal of the thermocouple from the furnace was rather difficult. After a suggestion by K. Watanabe a ground glass joint was designed so as to render this operation more easy and at the same time this change facilitated placing the thermocouple junction in its proper place.

Schematic Diagram of 2 mm Tube

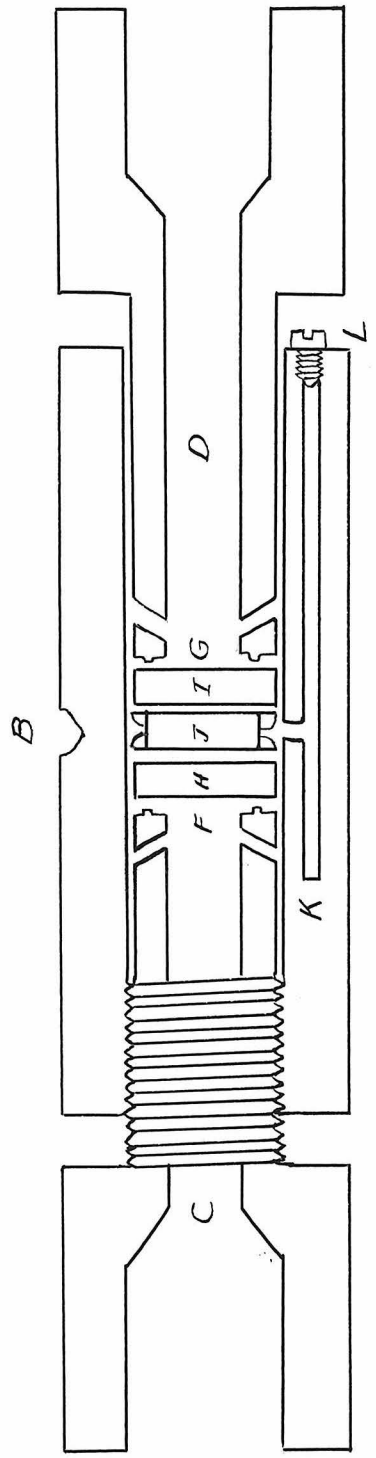

Fig. 1.

Two absorption cells were used. The first one which was used for low pressures of the absorbing Cs vapor was approximately 7.5 cm long and was constructed of copper. For the higher pressures a tube length of about 2 mm was used. The design* of the latter is somewhat different from that originally used by Ch'en and Watanabe so a brief description and drawing will be given here.

The steel cylinder A is provided with a cup B wherin the hot junction of the thermocouple fits. One end is threaded so that by turning the plunger C the elements F,G (copper gasket), H and I (Mg O window), and J (steel gasket) can be properly lined up. The cylinder A is also provided with a passage way K for the Cs which is sealed off by means of a copper screw L. The final seal is effected by applying pressure to the plunger D which fits snugly in the tube A. In so doing, the threaded plunger remains stationary while the elements F, H, J, I and G press upon each other until finally the copper gaskets F and G (previously annealed) collapse transversely toward walls of cylinder A, and longitudinally against the MgO windows H and I. The steel gasket J is about 2 mm in thickness and is provided with three holes together with a U cut around its outer walls so that the region J is in communication with the chamber K.

The advantages of the above design over that previously used are

* This tube was constructed and designed in collaboration with J. Pearson of the California Institute of Technology machine shop.

as follows. In the first place the movable parts F, H, J, I, G can be rather easily withdrawn from the cylinder A by unscrewing C and sliding D out. Then with the aid of a cylindrical bar of wood and a vise the elements can be easily removed without injuring the MgO windows. (This was rather impossible with the old design where the gasket J was built onto the tube A). In the second place the gasket J may be replaced with other gaskets of various lengths without having to make a new assembly.

It was found that the MgO windows whose durability in the presence of alkali vapors was first studied by R. T. Brice[53] were not appreciably attacked by the Cs vapor. At room temperature (because of impurities) Cs is liquid, hence no great difficulty was encountered in feeding the tube with Cs. The biggest difficulty was that of getting Cs into the absorption tube without spattering the windows with CsO which has the tendency of cutting down the transmission. This spattering came about in the following manner. In effecting the transfer of the Cs from the .1 gm capsules to the absorption tube the tube was first filled with xylol and the Cs was transferred (in case of the long tube) by means of the glass spoon into the tube. In this process some of the Cs becomes oxidized and floats upon the surface. Subsequent evacuation causes xylol to boil vigorously and in so doing the MgO windows at the ends of the tube obtain deposits of CsO. After a suggestion by Professor Bowen, this difficulty was removed by constructing a small copper cup which was filled with a little xylol and about a .1 gm of Cs and placed into the

tube. A little xylol was also placed within the tube proper to act as a flushing agent. During the process of putting the Cs into the tube N_2 was allowed to circulate freely within the system thus excluding as much air as possible. Thus, when it came finally to sealing the system only N_2 and xylol vapor which do not affect the Cs were present to any extent.

Before each run the absorption tube together with the elements comprising it was put in the furnace and heated to a temperature of about 500°C for 24 hours while at the same time maintaining the pressure at 2×10^{-5} mm Hg (measured by a McLeod gauge) so as to expel the occluded gases. The power for the furnace was supplied from the direct current generator in West Bridge which was provided with a voltage regulator keeping the voltage at 110 v. The temperature within the absorption cell could be kept at a temperature constant to within 1.5 degrees for an indefinite period - just so long as the vacuum system springs no leak.

3. Temperature Determination

To ascertain the temperature within the absorption cell the method of Lloyd and Hughes[1] together with the important improvement of Watanabe[2] was used. Watanabe's improvement consisted in obtaining metallic contact between the absorption cell and the hot junction of the thermocouple by means of a low-melting point alloy which he had prepared and which was used in the present work. This device cut down considerably the error of temperature measurement.

A new chromel-alumel thermocouple was constructed and calibrated

"in situ"[1),2)]. An optical arrangement was provided so that the melting point standard within the cell could be observed conveniently while at the same time manipulating the temperature of the furnace and making measurements of the thermal E.M.F. The optical system consisted simply of a plane mirror and a telescope together with a lamp to illuminate the metallic strips used for calibration within the cell. It was found necessary to construct and calibrate two thermocouples in as much as after completing Run #1 the junction broke. The characteristics of the second thermocouple were slightly different from that of the first. Nevertheless the first calibration could not be used. The calibration curves were fitted to a parabola by the method of least moments.[54)]

4. Spectrograph and Optical Arrangement

The light from the lamp was caused to pass through the absorption tube by means of a thin lense of focus 23 cm. After passing through the tube a second lense of focus 21 cm with the aid of a prism enabled one to focus the filament of the lamp onto the slit of the spectrograph. The spectrograph used consisted of a concave grating of 21 foot focal length and has a dispersion very close to 2.64 A/mm when the mounting is of the R owland type, which was the case here.[55)] The resolving power of the grating is approximately 70,000. In the case of the resonance lines of Cs a red Wratten F #49 filter was placed over the slit to cut off the second order violet.

The grating was adjusted for tilt and illumination by visual methods in the usual manner and also for focus photographically with the aid of an

iron arc. Before use the slit of the spectrograph was cleaned with alcohol. Also the grating, with the aid of Professor Bowen, was cleaned with alcohol and powdered chalk. The micrometer screw for the slit was found to exhibit a lag -- in particular it was found that the zero setting is -3 u instead of zero.

5. a. Photometry. General Considerations

Perhaps the greatest source of error in the study of line contours can be attributed to the photometry. In principle the method consists of correlating the blackening of a photographic plate with the intensity of the light incident upon it. Now in view of the limitations engendered by the use of a Rowland spectrograph Lloyd,[1] Watanabe,[2] and Ch'en[3] undertook to study the intensity distribution of their respective lines of interest in the following manner:

A step weakener consisting of 13 steps is placed in a position just before the plate in the plate holder which position it has when used later. Sections of the plate are then subject to equal exposure times, the amount of light reaching the plate being ascertained by the transmission of a rotating sector which is placed before the slit. Then by taking microphotometer traces transversely across the sections and longitudinally along the steps where the transmission of the rotating sector is unity the transmission of the various steps can be ascertained. Corrections, of course, are made for the varying sensitivity of the plate with wave length.

Now several possible sources of error in the calibration of the step weakeners are present (neglecting that due to the relative position of

the absorption lines from the stepweakeners) (a) In the above method it is assumed that the intrinsic intensity of the source remains constant for each exposed strip. This may not be so, in fact as time progresses the temperature of the filament increases as is indicated by a dropping of the amperage, since a drop in the current assuming that the voltage is constant (moreover, here is another difficulty) means an increase of resistance. Considering the relatively short time (about an hour) required to expose the various strips this source of error may not be large but it is certainly there. (b) Furthermore it is assumed that the intermittent exposure effected by the rotating sectors is equivalent to a continuous exposure as given by the transmission of the sectors. Until rather recently some uncertainty existed. However it has been shown by various workers, for example J. H. Webb[56] that an intermittent exposure is equivalent to the corresponding continuous one provided the frequency of flash is above some minimum critical value which depends on the type of emulsion used and the intensity of the source. (c) Also the various sections are not exposed simultaneously so there exists another source of error, namely, the "latent image" effect whereby the latent image produced by photons incident on the plate is subject to a growth or decay as time passes. Thus when the plate is developed, the blackening of the various sectors are not that assumed. This effect has been studied by various authors.[57]

The above mentioned errors are of such nature that they cannot be entirely eliminated using the method described above. No mention was

made of the fact that a large error is introduced by the circumstance that the various steps of the step weakener cover a considerable wave length region which introduces discrepancies in the study of the absorption contours in spite of interpolation means to cut it down. Consequently it became necessary to find a different and perhaps more accurate way of photometric procedure.

b. Astigmatic Photometry

Now the geometry of the Rowland grating is such as to render intensity measurements by utilizing the astigmatic nature of the image on the plate. (See Appendix) This astigmatism manifests itself in the following way. The spectrum produced by the grating has a constant intensity near the center and as one proceeds towards the ends the intensity falls off in a calculable manner: (1) If the intensity distribution along the slit length is known and (2) if the grating is uniformly reflecting. One can, then, for any part of the spectrum obtain calibration marks without any auxiliary apparatus. This method of astigmatic photometry was first suggested by G. H. Dieke[5] and later was actually subject to extensive tests by M. I. Bresch[6] who applied the method to the study of the relative intensities of line spectra where it was found that the astigmatic method compared very favorably with others.

It is obvious that the errors inherent in the calibration of the step weakener are absent. Nevertheless to check the feasibility of the autocalibration method the step weakeners used by Lloyd,[1] Watanabe,[2] and Ch'en[3] were calibrated via the astigmatism method. The transmissions

(A) are the values obtained by astigmatism. (B) and (C) are the transmissions obtained by the rotating sector methods. The former were ascertained by Watanabe and the latter by Lloyd:

Step	(A) % Trans.	(B) % Trans.	(C) % Trans.
1	96.8	96	98
2	88.6	86	90
3	78.7	81.5	85
4	71.0	78	80
5	66.7	72	73
6	60.5	66	65
7	51.3	56	55
8	45.4	47	45
9	34.3	38	35
10	31.2	30	25
11	22	18	17
12	13	10	12
13	7.5	6	10

On the whole the agreement is fairly good except for steps 4, 5, 6 and 7 where (B) and (C) deviate quite considerably from (A), the average deviation being about 10%. Fortunately however in subsequent calculations the log of the transmission is used, hence, in the final results the error is considerably less. In the calibration of the

step weakeners by the astigmatism method it was found that the transmissions of various parts of the step were different by as much as 5%.

c. Assumptions Made in the Calculation; Verification of Conditions.

In deducing the formulae pertinent to the autocalibration method three conditions must be satisfied: (1) Each ruling of the grating must be such that the contribution of every point along its length to the intensity of the line be equal (5). (2) The grating must be filled with light vertically in a uniform manner. (3) The slit must be exactly parallel to the rulings of the grating. These requirements are obvious as the derivation of the formulae show.

Now from appendix (I) we have from the theory for the total length of the image and that of the constant portion

$$L_T = L \sin \phi \tan \phi + \frac{s}{\cos \phi}$$
$$L_C = L \sin \phi \tan \phi - \frac{s}{\cos \phi} \qquad (1)$$

where L is the length of each ruling of the grating, s the length of the slit and ϕ the angle of incidence of the light on the grating. The requirement (3) above for the grating is necessary even in the absence of astigmatism and was readily shown to be satisfied by taking iron arc pictures and examining the definition of the image. The requirement (2) can readily be fulfilled. The success or failure of the astigmatism method hinges principally on requirement (1). To show that it held for

the grating used a picture was taken with the slit reduced to a point source and a microphotometer trace was made of the astigmatic image. The microphotometer trace showed that the intensity distribution was rather constant over the whole length of the image. From this it was concluded, since from (1) the slit length plays no role, that the lines of the grating taken as a whole satisfy condition

In the study of the red Cs lines an aperture for the grating and decker for the slit were designed so as to give as large an image as possible with as small as possible central portion consistent with limitations of measurement and width of usable plate. The length of the effective rulings of the grating and the length of the slit were

$$\begin{aligned} L &= 3.837 \text{ cm} \\ S &= .907 \text{ cm} \end{aligned} \qquad (2)$$

The angle of incidence, in case of the resonance lines of Cs was

$$\begin{aligned} \phi &= 30^\circ\ 50'\ 45'', \text{ hence} \\ \text{Tan } \phi &= .5972 \\ \text{Sin } \phi &= .5127 \\ \text{Cos } \phi &= .8586 \end{aligned} \qquad (3)$$

The angle of reflection could be safely put equal to zero since only an error of one part in a thousand would result from this assumption in making calculations of the L_T and L_C. If we put (2) and (3) in (1)

one obtains for L_T and L_C the following values:

$$L_T = 2.232 \text{ cm}$$
$$L_C = .120 \text{ cm} \qquad (4)$$

d. The Astigmatism Calibration Curve and Its Utilization

Now, if a microphotometer trace is taken transverse to the direction of increasing or decreasing wave length the following type of curve is obtained as shown in the figure (2). Along side of it an example of an absorption contour is shown which is obtained by taking a microphotometer trace parallel to the direction of λ . In taking the astigmatism trace care must be taken so that the maximum AA' corresponds as closely as possible to "no absorption" which is the point, say, A" in the figure. Now the problem remains of correlating the galvanometer deflection G (as recorded by the microphotometer plates) of the calibration curve with the transmission. This is done in the following manner. From the calculated lengths of the total and constant portion of the astigmatism distribution and the magnification of the trace (it was 6:1 for all plates used in the present work) the curve BDD'B' could be constructed. From this curve the transmission as a function of the galvanometer deflection is readily obtained. For example if we wish to find the transmission corresponding to the point G' it is only necessary to draw a line G'T parallel to OG_c. Its intersection T with BD gives one the transmission; it being merely the ratio of TF to

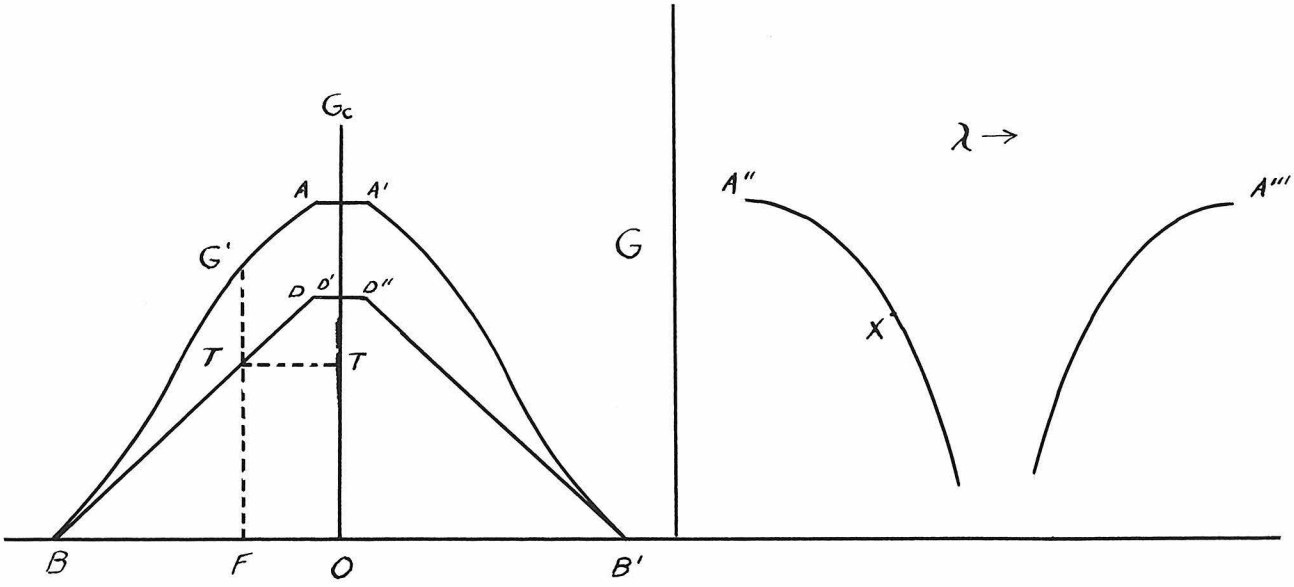
G_c
A
A'
G'
D
D'
D''
T
T
G
$\lambda \rightarrow$
A''
A'''
X'
B
F
O
B'

FIG. 2

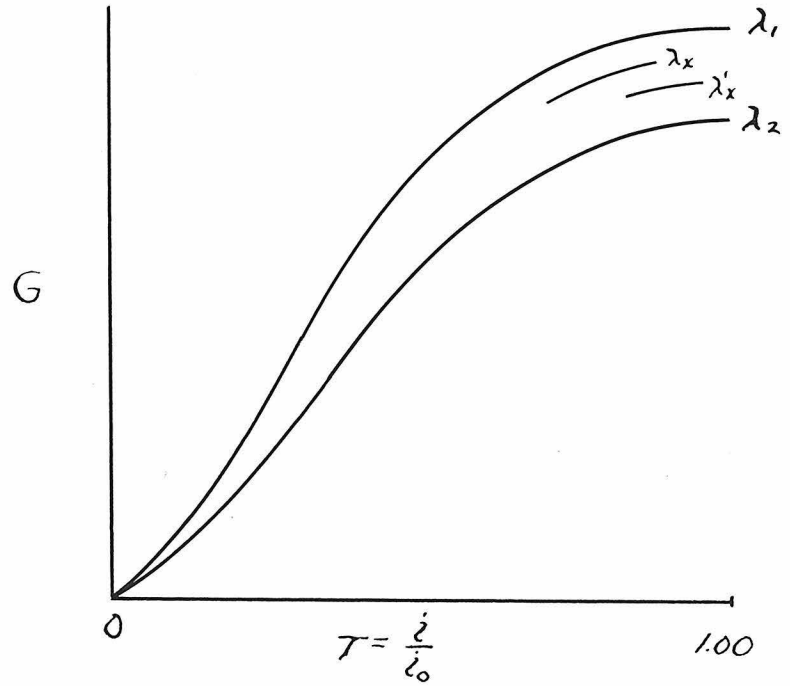
λ_1
λ_x
λ'_x
λ_2
G
0
$T = \frac{i}{i_0}$
1.00

FIG. 3

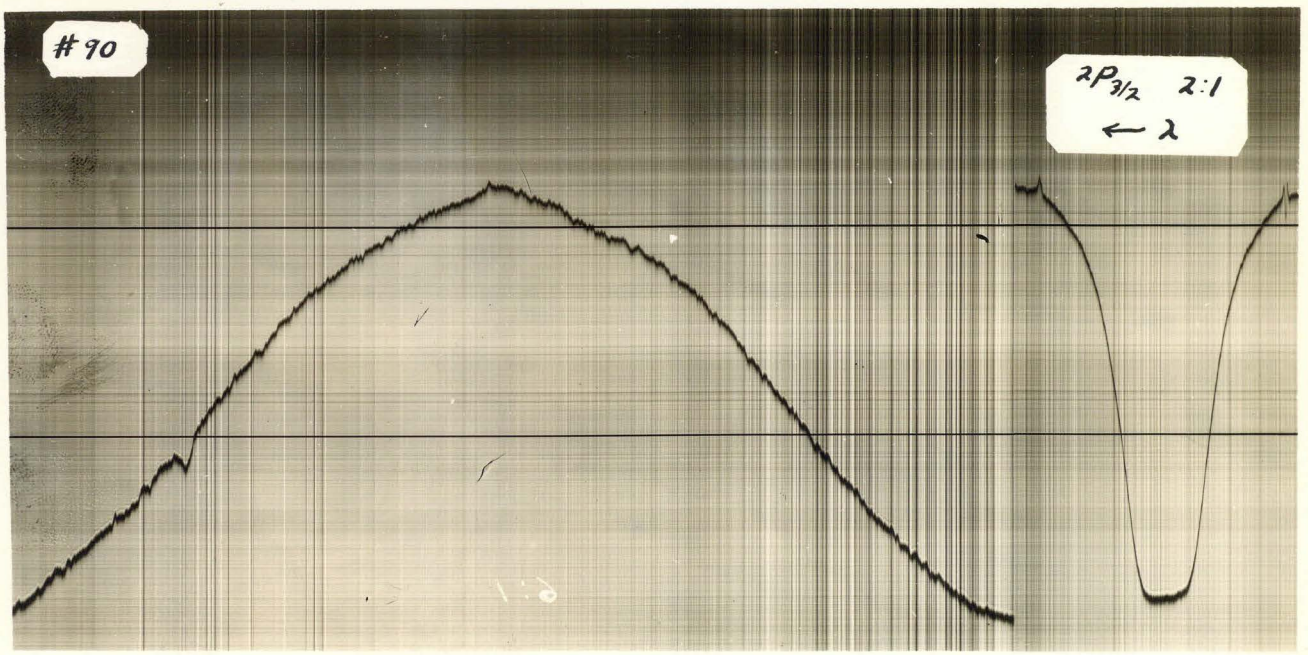

Example of Microphotometer

Line and Astigmatism Trace

OD'. This procedure is then repeated for the other points of the trace. Knowing the transmission as a function of the galvanometer deflection the transmission of any point X of the absorption contour can be readily obtained.

In the above it was assumed that the sensitivity of the plate is uniform, so that the trace at A" is the same as that at A"'. In most cases this is not the same so that the calibration curve at A" only holds, strictly speaking, for the point A" on the contour. The transmissions at the intermediate points in the interval A"A"' are obtained by taking an astigmatism trace through A" and A"', obtaining then the transmissions as a function of the galvanometer deflections and the two wave lengths corresponding to the points A" and A"', say λ_1 and λ_2. Curves of the nature shown in figure (3) are constructed. The transmissions at wave lengths intermediate to the wave lengths λ_1 and λ_2 are then obtained by linear interpolation, which is best done graphically, but also can be done analytically if it is so desired.

e. Photography and Related Matters

For the first members of the principal series of Cs[59] $\lambda_{^2P_{3/2}} = 8521.12, \lambda_{^2P_{1/2}} = 8943.46$ Eastman IP plates were used. In the neighborhood of the $^2P_{3/2}$ component the sensitivity of the plate was quite constant and could be considered so for the rather narrow lines. On the other hand in the region of the $^2P_{1/2}$ component the sensitivity varied considerably, it being rather impossible to study

the broadening at the higher pressures (P > 15 mm Hg). Besides being less uniform the average sensitivity was very much less in this region also.

Before use the plates were hypersensitized in a 4% solution of NH_4OH. At first it was rather difficult to hypersensitize the plates uniformly. It was found, however, that the following procedure is conducive to uniformity. The NH_4OH solution is first chilled to a temperature of approximately 11°C and is placed in a cylindrical glass vessel of 6 cm diameter, and 30 cm height. The plate (22 cm long) is then placed into the solution and agitated continually for about 70 seconds. One end of the plate is then placed in contact with a paper towel lying flat on a bench close by. After "dabbing" the one end on the paper towel three or four times the plate is placed in a dryer (of the electric fan type) for an hour (this being the time required to thoroughly dry the plate).

To acquire a workable density on the plate an average exposure of 8 hours was required when the slit of the spectrograph is 20 microns wide. This, as was mentioned before, holds when the lamp is operating at about 80 amps, several filament changes being also required. It is advantageous to operate the lamp in such manner as to decrease the exposure time compatible with work necessary to change filament since this cuts down the resultant fog of the background considerably. After sensitization the I-P plates have a tendency to fog on standing.

After exposure the plates were developed for 5 minutes with D-11 Eastman developer and fixed for about 15 minutes in Eastman F-1 fixer. Both the fixer and developer were at a temperature of 18°C. While developing, the plates were brushed with a camel's hair brush. After fixing the plates were washed for a half hour in running water and dried. On the whole the final plates showed a rather uniform character.

IV. Experimental and Theoretical Synthesis. Measurements.

1. Microphotometer

The microphotometer used was of the Kruss type. The magnification ratios were 2:1, 6:1, and 40:1 according to the manufacturer but it was found that the last ratio was in reality 39.6:1. The slit widths used were 20 microns for the narrow lines and 30 microns for the wider ones. Because the astigmatic method was used it was necessary to choose effective slit lengths a little smaller than the width of the constant portion of the astigmatism calibration curve, the width chosen was somewhat less than a millimeter. All of the astigmatism traces were magnified in a ratio of 6:1 whereas the contour traces where subject to different magnification ratios according to the particular circumstance.

After obtaining the microphotometer plate and after following a suggestion from Professor Bowen it was thought to be of sufficient accuracy to reproduce the trace on millimeter graph paper by merely placing the paper on the microphotometer plate, which was situated on a ground glass surface properly illuminated, and tracing the line contour and astigmatism curve with a sharp pencil. This expedient saved much time and is rather satisfactory. Not much added accuracy is obtained if a comparator is used because of the somewhat erratic micro-deflections due to the inherent graininess of the photographic plate. Besides, the widths of the lines and the astigmatism traces rendered measurements by the comparator somewhat superfluous. Also, because of the non-uniformity of hypersensitiza-

tion one cannot be sure that the measurements are not spurious, to say the least.

The contours were then subject to the method described in III-5-d, to obtain i/i_o as a function of the wave length for the line contours. For the narrow lines the transmission i/i_o for the whole contour was ascertained. For the wider lines only the wings of the lines were studied where i/i_o ranged from $\simeq$ 1.00 to $\simeq$ .3. As it was pointed out in III - 5 some uncertainty existed as to the estimation of the background: $(i/i_o = 1)$.

2. Vapor Pressure

Although much data existed regarding the vapor pressure of Cs as a function of temperature it was thought that the rather recent determination of the vapor pressure-temperature relation of Langmuir[60] and associates was more reliable than the others. The empirical formula

$$\log_{10} p_{mm} = 11.0531 - 1.35 \log_{10} T - \frac{4041}{T} \cdots \qquad (1)$$

was used throughout, where p_{mm} is the vapor pressure in mms of Hg, and T is the absolute temperature. The above holds for equilibrium between the liquid and gaseous state of Cs. The range of validity is from $T = 350^{\circ}K$ to $600^{\circ}K$ with an accuracy of 2% in this range.

Knowing the temperature and consequently the vapor pressure as given by (1) it is not difficult to show that if the perfect gas law is assumed, the number of Cs atoms per unit volume is given by

$$N = 9.71 \times 10^{18}\, p_{mm}/T \qquad (2)$$

3. Experimental Evaluation of γ

Two cases are to be distinguished here. Namely the case of the narrow lines ($p_{mm} \leq 10^{-2}$) and the wide lines ($p_{mm} > 10^{-2}$).

a. Narrow Lines

In this case because of insufficient resolution of the spectrograph and microphotometer due to finite slit width, the contour can not be adequately compared with a theoretical one without knowing a priori the effect of the finite slit width. Here, however, resort to the method of total absorption[61] can be made which is independent of the resolving power characteristics of the instruments used to study the line. Now if we assume a dispersion distribution such as that in I-2.(1) and utilize I-1.(2),(7) and (8), we obtain

$$\alpha\chi = -\log_e i/i_o = \frac{KX\,\gamma/2\pi}{(\Delta\nu)^2 + '(\gamma/2)^2} \qquad (3)$$

where

$$K = \frac{\pi e^2}{mc} Nf \qquad (4)$$

According to Ladenburg and Reiche[61]

$$\int_{-\infty}^{\infty} (1 - \frac{i}{i_o})\, d\Delta\lambda = \text{const} = A \qquad (5)$$

which assertion had been tested by Minkowski[62]. Putting (3) in (5) and integrating one obtains

$$C = 3.46 \times 10^{-18}\ \text{Å}^2 \quad ^{2)} \tag{6}$$

where

$$C = \frac{\lambda_o^4 e^2 N f \chi \gamma}{2mc^3 \log_e 10} \tag{7}$$

In (6) the Å is measured in angstrom units. Consequently the knowledge of f and A enables one to obtain γ if a dispersion distribution is assumed, which assumption shall be subject to a test. For the $^2P_{3/2}$ and $^2P_{1/2}$ lines of Cs we have for the f-values respectively .66 and .32[13] so that (7) becomes if we denote the $^2P_{3/2}$ by the subscript 1 and the $^2P_{1/2}$ by the subscript 2 or by s and 1 respectively then (7) becomes

$$\begin{aligned} 10^{40} \chi C_1 &= .707\ N \chi \gamma_1 \text{ or } \gamma_s \\ 10^{40} \chi C_2 &= .416\ N \chi \gamma_2 \text{ or } \gamma_\ell \end{aligned} \tag{8}$$

where we shall interchange 1 and s or 2 or 1, occasionally, both notations being equivalent. So much, then, for the rather narrow lines.

b. Wide Lines

For pressures greater than 10^{-2} mm Hg we resort to the so-called "straight line" method. Here again we utilize the dispersion formula (3) which according to I-2b is valid at the wings of the line. (3) can be readily put in the form

$$(\Delta\lambda)^2 = C\left(\log_{10} i_0/i\right)^{-1} - \gamma^2 \lambda_o^4 / 4C^2 \tag{9}$$

where C is given by (8) for the $^2P_{3/2}$ and $^2P_{1/2}$ components respectively.

In using (9) the term $-\gamma^2\lambda_o^4/4C^2$ can be neglected, since it has no appreciable effect on the final results. Examination of (9) discloses, then, that if one plots $(\Delta\lambda)^2$ against $(\log_{10} i_o/i)^{-1}$ a straight line results whose slope is C and which passes essentially through the origin. Consequently, the ascertainment of this slope enables us to obtain γ_1 and γ_2 by means of (8).

c. Asymmetry and Shift

For $p_{mm} > 1$ mm Hg asymmetries were evident. Attempts were made to fit the contours to the "-3/2" type of curve exemplified by I-2.(18). This attempt proved futile, so that both wings of the lines were subject to the same tests and considerations in (b). Also the experimental absorption contours were drawn.

Because of total absorption at the center of the line it is rather impossible to measure the shift so that no consideration is given to this phase here. Under ideal conditions the shift could be measured if a short enough workable absorpiton tube could be constructed which would tend to cut down the absorption at the line center.

4. Experimental Results

Utilizing the method of calculation outlined in 3, the values of C_1, C_2, γ_1, and γ_2 given in table I were obtained. In all, three successful runs were made. However, in run #2 the temperature determination was not quite correct because it was found that the thermocouple junction was not in its proper position after the run was completed. Nevertheless the results are useful in the evaluation of γ_1/γ_2 which

Table I

Run #1, X = 7.25 cm

#	T	P_{mm} Hg	N	C_1
54	414.0	5.75×10^{-3}	1.35×10^{14}	1.49×10^{-18}
55	429.9	1.26×10^{-2}	2.64×10^{14}	6.89×10^{-18}
56	460.8	5.01×10^{-2}	1.05×10^{15}	9.27×10^{-17}
57	490.0	1.59×10^{-1}	3.12×10^{15}	8.27×10^{-16}
58	512.4	3.16×10^{-1}	6.00×10^{15}	2.33×10^{-15}

Run #2, X = 7.00 cm

70				2.02×10^{-18}
72				6.90×10^{-18}
79			(?)	1.34×10^{-17}
80				1.43×10^{-16}
74				1.61×10^{-16}

Run #3, X = .1905 cm

87	512.2	.334	6.46×10^{15}	$.905 \times 10^{-16}$
88	532.6	.640	1.16×10^{16}	3.01×10^{-16}
89	564.8	1.60	2.74×10^{16}	1.50×10^{-15}
90	583.9	2.47	4.11×10^{16}	2.50×10^{-15}
91	609.7	4.71	7.50×10^{16}	6.81×10^{-15}
92	672.7	17.50	2.52×10^{17}	3.84×10^{-14}

Table I (continued)

C_2	γ_1	γ_2	$/N \times 10^7$	$/N \times 10^7$	γ_1/γ_2
6.00×10^{-19}	1.70×10^7	1.07×10^7	1.26	.79	1.60
2.40×10^{-18}	4.60×10^7	2.59×10^7	1.74	.98	1.78
2.87×10^{-17}	1.73×10^8	9.11×10^7	1.65	.87	1.90
3.44×10^{-16}	5.16×10^8	3.64×10^8	1.65	1.17	1.415
5.21×10^{-16}	7.56×10^8	2.86×10^8	1.26	4.76	2.65
8.30×10^{-19}					1.43
2.52×10^{-18}					1.61
4.56×10^{-18}		(?)			1.74
3.88×10^{-17}					2.17
5.16×10^{-16}					1.92
$.376 \times 10^{-16}$	1.07×10^9	7.55×10^8	1.30	.915	1.42
$.683 \times 10^{-16}$	1.93×10^9	7.45×10^9	1.67	.58	2.58
5.26×10^{-16}	4.05×10^9	2.51×10^9	1.48	.92	1.61
1.17×10^{-15}	4.31×10^9	3.60×10^9	1.04	.87	1.20
3.25×10^{-15}	6.75×10^9	5.35×10^9	.90	.71	1.26
?	1.02×10^{10}	?	.41	?	?

is independent of the temperature, or N. For the lower pressures ($\lesssim 10^{-2}$) the γ obtained experimentally is corrected for natural breadth according to the circumstance of the addivity of the breadths due to the two causes, see I-2.(18) for example. The experimental natural breadths[63] used were

$$\begin{aligned} \gamma_{N1} &= .479 \times 10^7 \\ \gamma_{N2} &= .419 \times 10^7 \end{aligned} \tag{1}$$

as compared with the theoretical values[64]

$$\begin{aligned} \gamma_{N1} &= .471 \times 10^7 \\ \gamma_{N2} &= .430 \times 10^7 \end{aligned} \tag{2}$$

It was found that for pressures below $\sim$ 1 mm Hg the lines were rather symmetrical in compliance with the theory. For pressures $>$ 1 mm Hg the lines exhibited asymmetry. C_1 and C_2 for both wings of each line were obtained and averaged. Also the straight lines for each wing are obtained and depicted graphically in figures. At the higher pressures band like structures at the wings of the line introduced difficulties of measurements.

Averaging the results of the table we obtain, leaving out runs #91 and #92, the following results:

$\gamma_1 / N \times 10^7$	$\gamma_2 / N \times 10^7$	γ_1 / γ_2
1.45	.84	1.8

where we have used the results of run #2 in the average for making a slight correction for the natural breadth for small c values according to the results of run #1.

5. Discussion of Line Contours

Two cases are to be distinguished, namely, the case for low pressures (< 1 mm of Hg) and that for high pressure (p > 1 mm). In the first case it was found experimentally that the broadening was essentially symmetrical and the plots of $(\Delta\lambda)^2$ vs $-(\log \frac{I}{I_o})^{-1}$ were fairly linear. This was the case for plates #54 to #58 and #70, #72, #79, #80, #74 where the pressure ranged from 10^{-2} mm Hg to 10^{-1} mm Hg. On the other hand for plates #87 to #92 the contours* seemed to show irregulatities at the wings of the lines which may be attributed to several causes:

(1) The irregularities are attributable to the inherent characteristics of the absorption lines.

(2) The irregularities may be due to the bands of Cs_2.

(3) The irregularities may be due to the nonuniformity of sensitization of the plates.

(4) The irregularities may be due to the nonuniform sensitivity of the plates.

These irregularities had the following characteristics. The red and violet sides of the $^2P_{3/2}$, and $^2P_{1/2}$ components seemed to have in general one or more "humps" at the extreme portion of the wings. The contour near the center of the lines was quite symmetrical in most cases but deviated considerably from symmetry for plate #90 $^2P_{1/2}$ and for plate

* See following pages for contours and or "straight lines" for plates #87, 88, 90, 91, and 92.

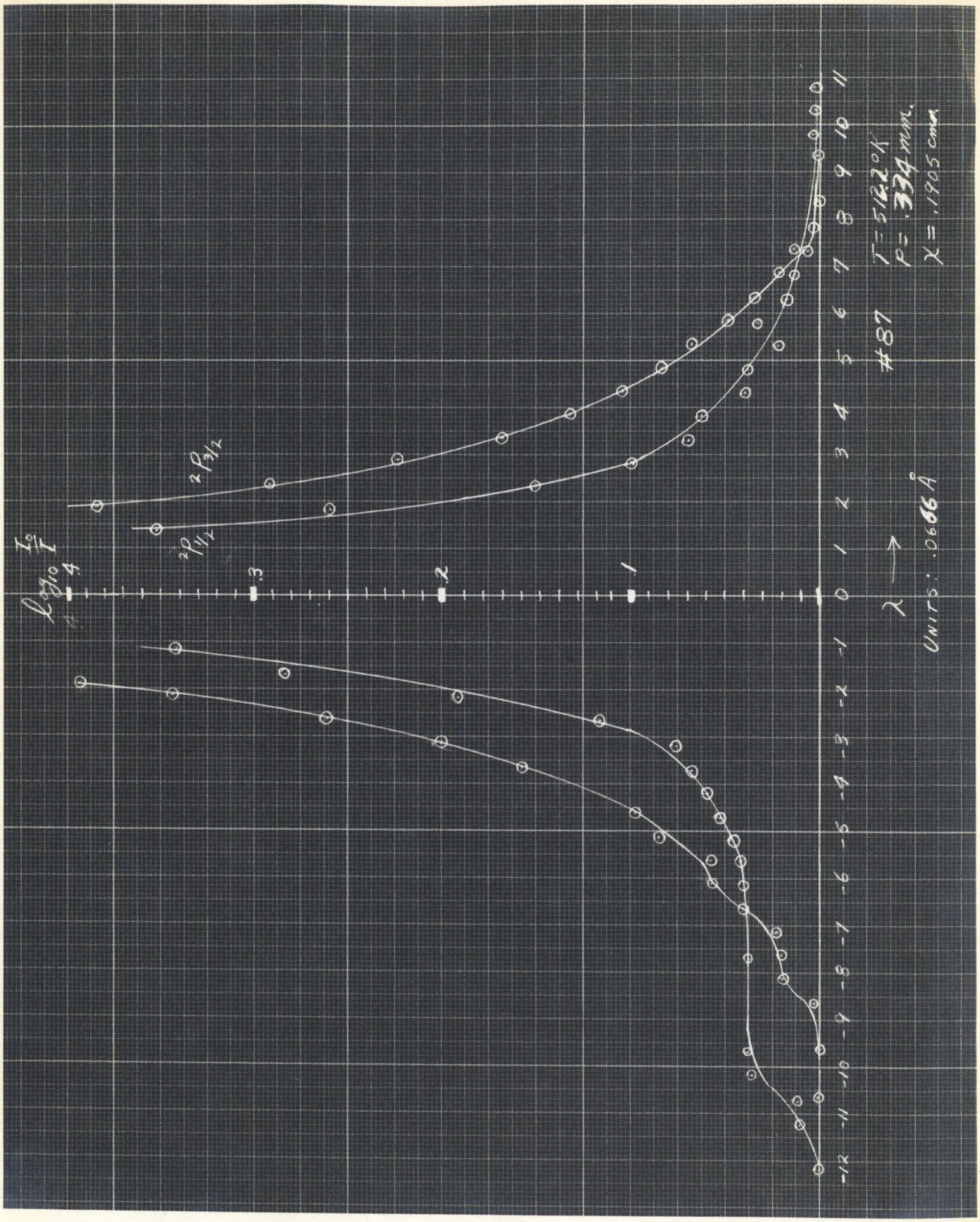
#87 T=562°k
p= 334 mm.
x = .1905 cm.
UNITS: .0666 Å
λ
-12 -11 -10 -9 -8 -7 -6 -5 -4 -3 -2 -1 0 1 2 3 4 5 6 7 8 9 10 11
1
.2
.3
.4
log10 I/I0
2P3/2
2P1/2

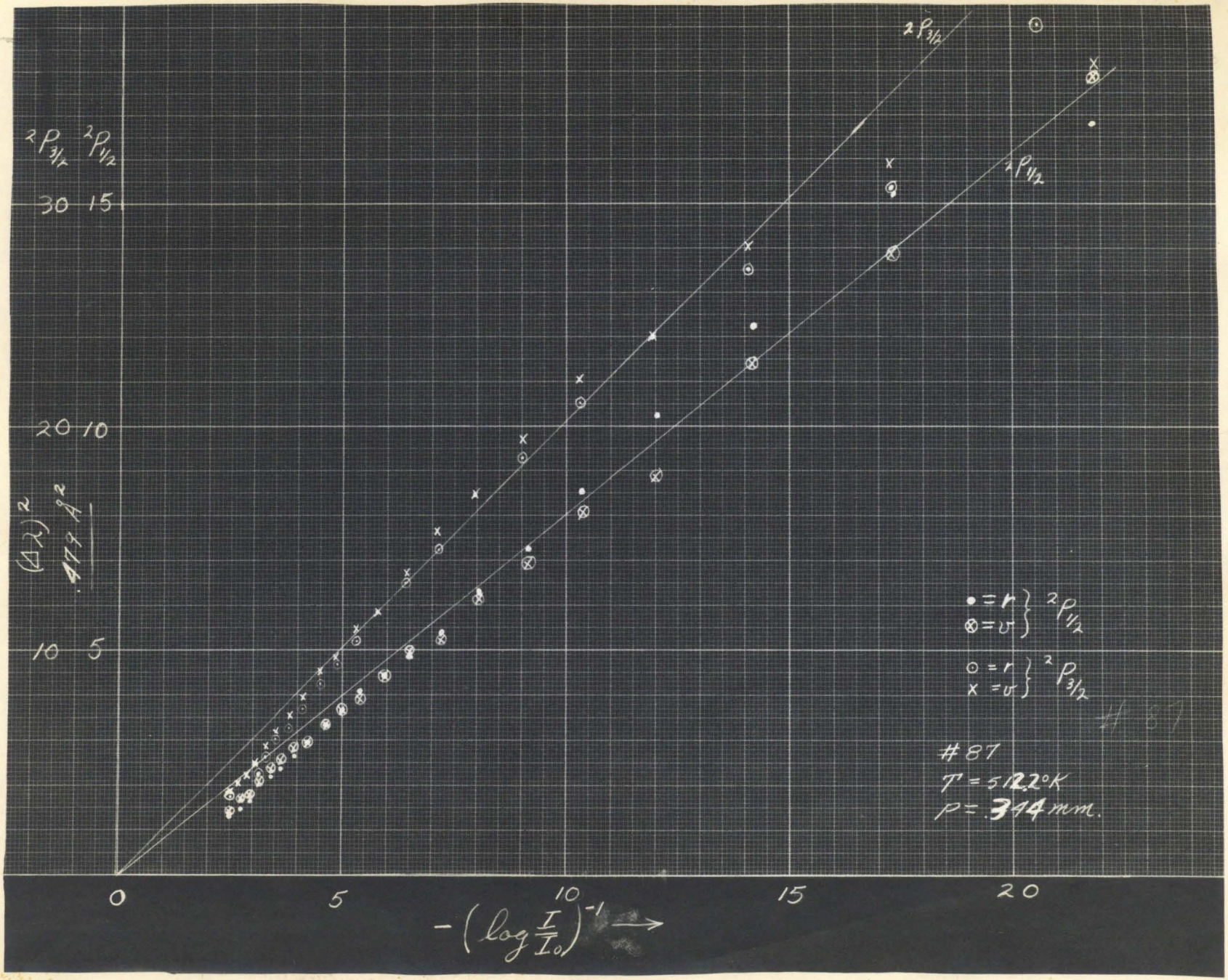
$^2P_{3/2}$ $^2P_{1/2}$
30 15
20 10
10 5
$\frac{(\Delta\lambda)^2}{4\pi^2\lambda^2}$
$^2P_{1/2}$
$^2P_{3/2}$
● = r } $^2P_{1/2}$
⊗ = v }
⊙ = r } $^2P_{3/2}$
× = v }
#87
T = 512.2°K
P = .344 mm.
0
5
10
15
20
$-\left(\log\frac{I}{I_0}\right)^{-1}$

$^2P_{3/2}$
$^2P_{1/2}$
$\log_{10} \frac{I_1}{I_2}$
4.
3.
2.
1.
0
1
2
3
4
5
6
7
8
9
10
11
12
13
V

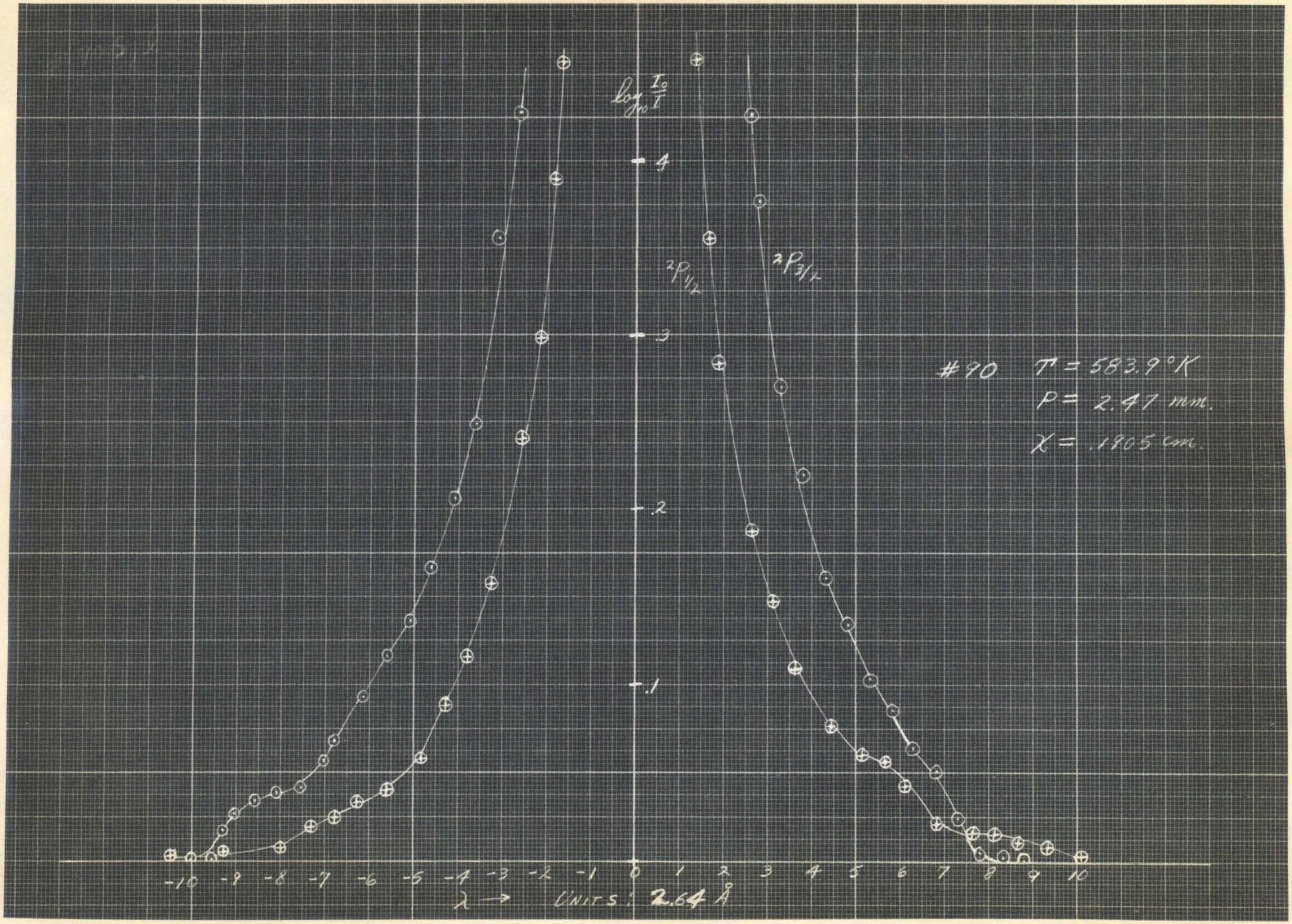
$\log_{10}\frac{I_0}{I}$
.4
.3
.2
.1
$^2P_{1/2}$
$^2P_{3/2}$
#90 T = 583.9°K
P = 2.47 mm.
χ = .1905 cm.
-10 -9 -8 -7 -6 -5 -4 -3 -2 -1 0 1 2 3 4 5 6 7 8 9 10
λ → UNITS: 2.64 Å

694

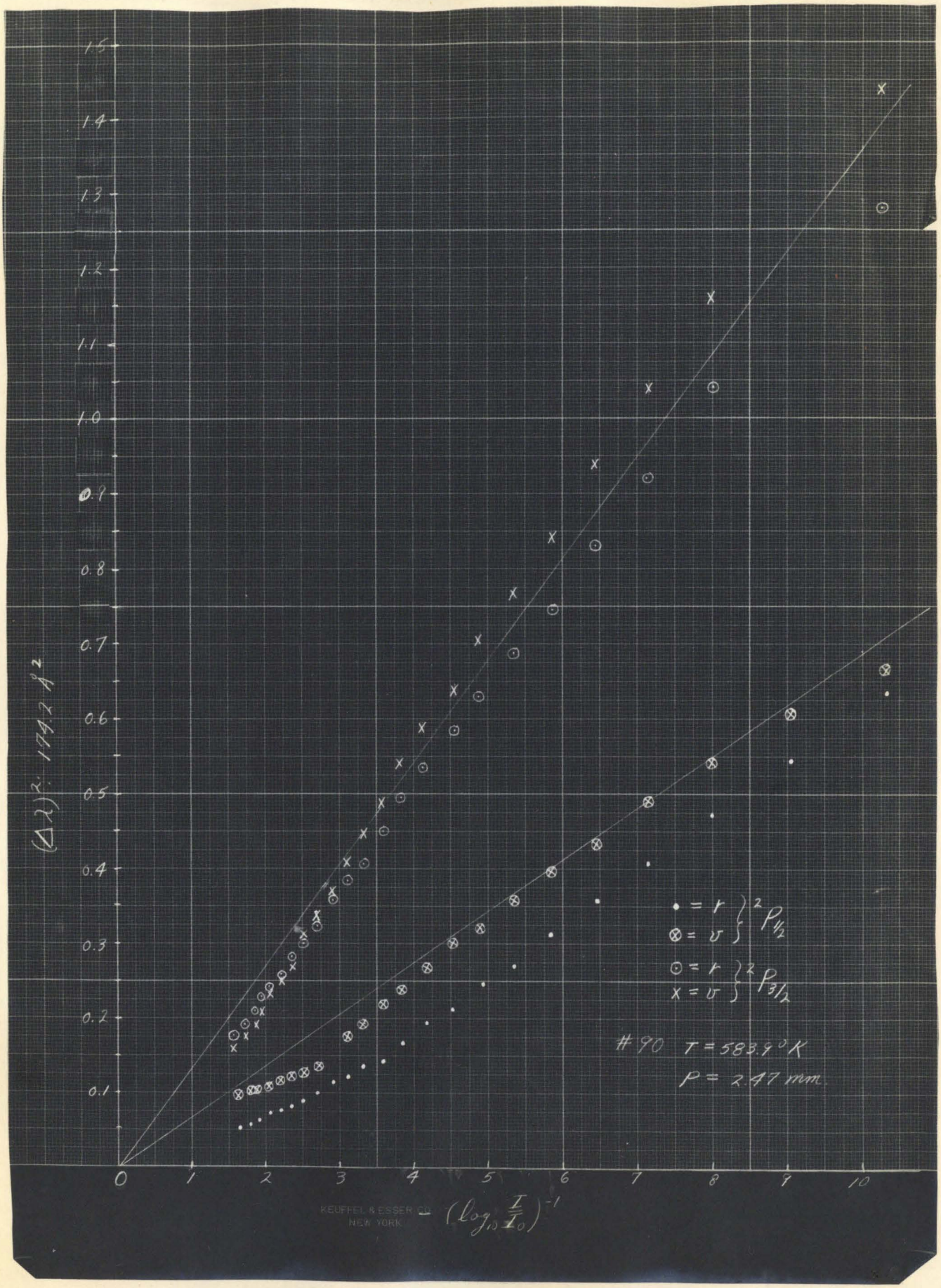
(Δν)² · 1742 Å²
(log₁₀ I/I₀)⁻¹
• = r } ² P 1/2
⊗ = v }
⊙ = r } ² P 3/2
X = v }
#90 T = 583.9°K
P = 2.47 mm
KEUFFEL & ESSER CO
NEW YORK

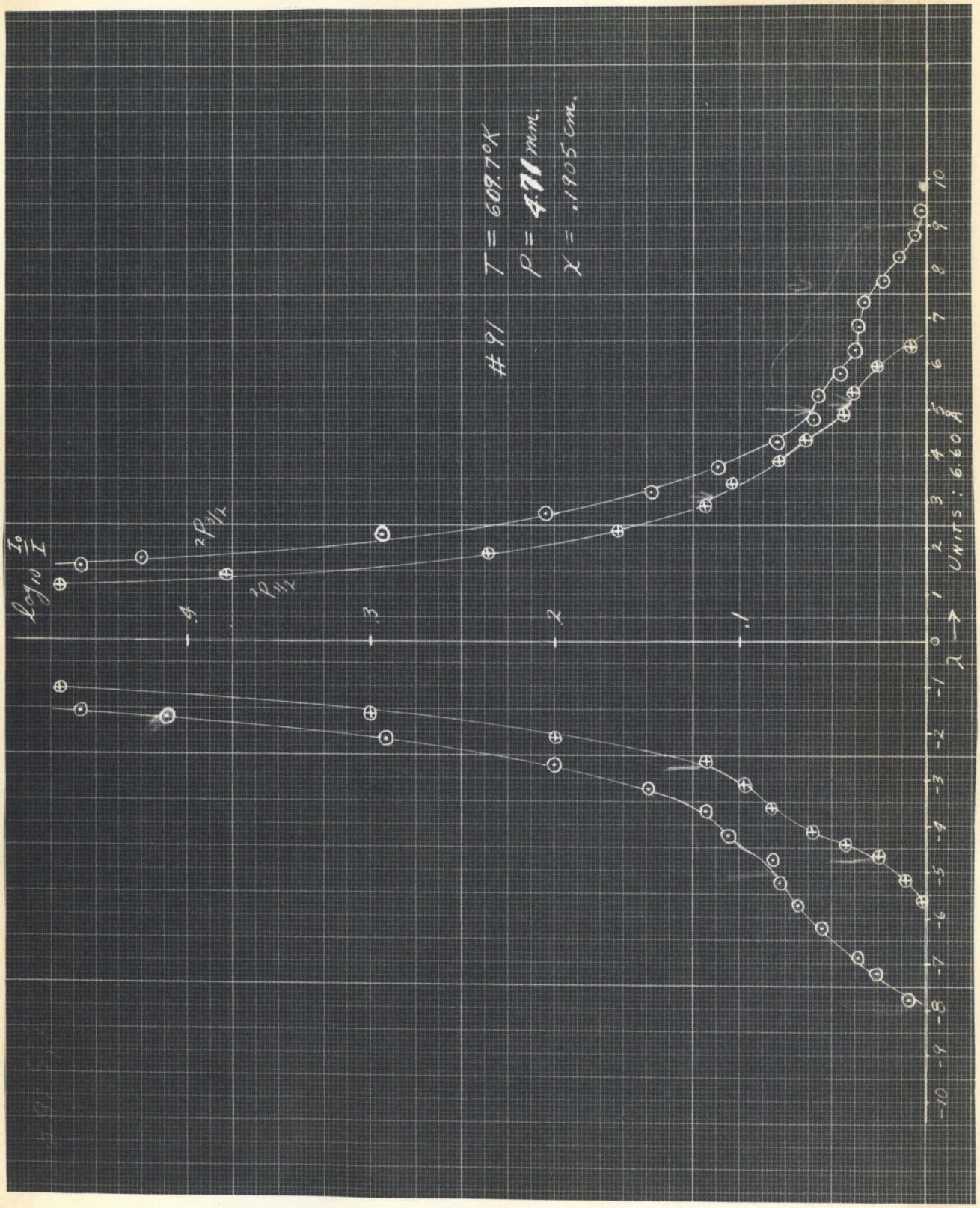
#91 T = 609.7°K
P = 4.11 mm.
x = .1905 cm.
$\log_{10} \frac{I_0}{I}$
2P3/2
2P1/2
UNITS: 0.6994
x

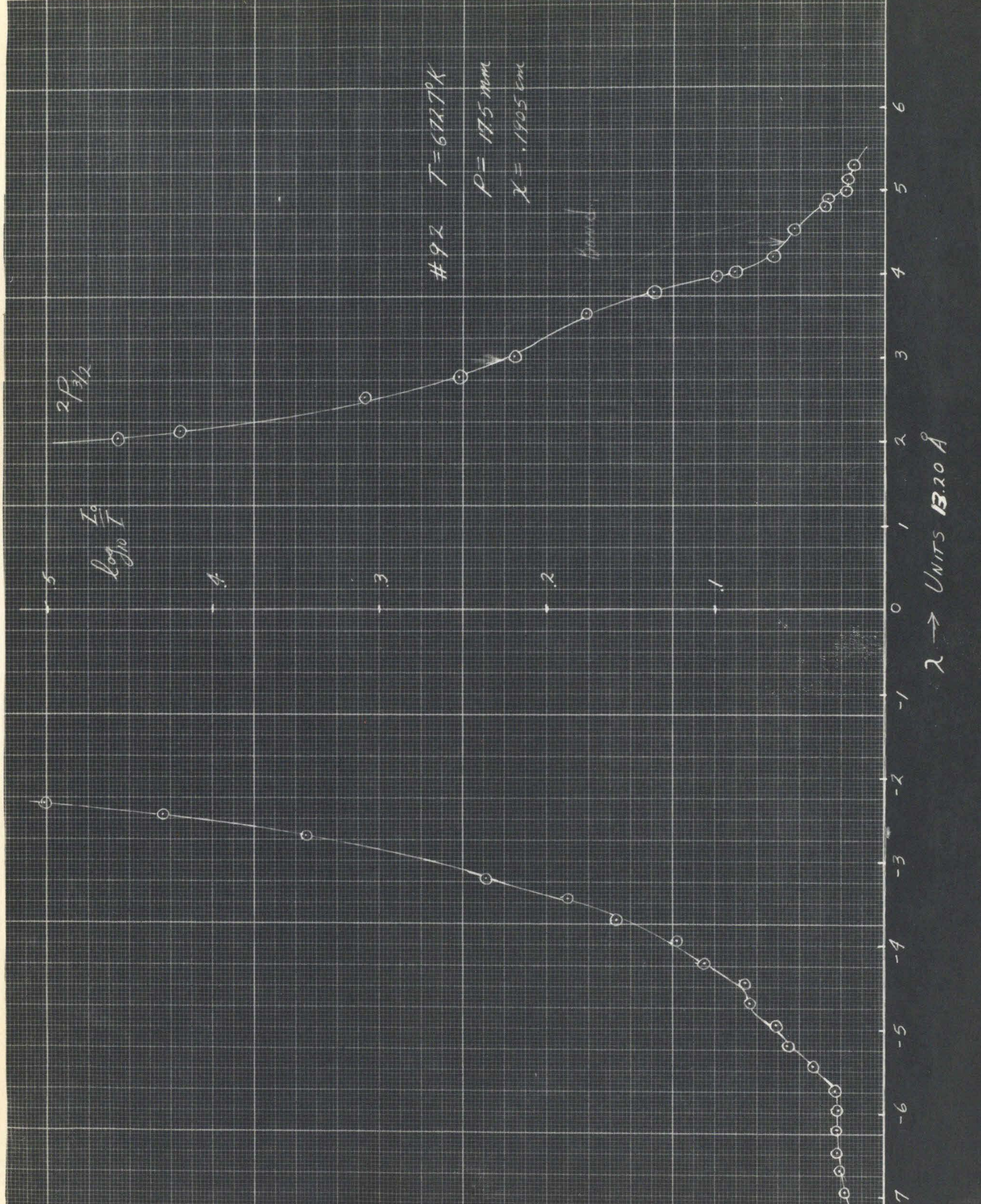
2P3/2
$\log_{10} \frac{I_0}{I}$
#92 T=672.7°K
P=17.5 mm
x=.1905 cm
λ → UNITS B.20 Å
.5
.4
.3
.2
.1
-7
-6
-5
-4
-3
-2
-1
0
1
2
3
4
5
6

#92 $^2P_{3/2}$ (the $^2P_{1/2}$ could not be studied since the red wing of the $^2P_{1/2}$ component covered a range which included the wave length region where the sensitivity of the plate was practically nil). The fact that near the center of the line plate #91 showed no appreciable asymmetry and the $^2P_{3/2}$ component for plate #90 showed no asymmetry leads one to suspect that the asymmetry of the $^2P_{1/2}$ component for plate #90 is spurious and can be attributed to errors arising in correcting for the non-uniform sensitivity of the plate in the region of the $^2P_{1/2}$ component where it increases considerably as the lines become broader and broader. The plot of $(\Delta\lambda)^2$ vs $-(\log_{10} \frac{I}{I_0})^{-1}$ is shown in the figure where it is seen that the straight line passing through the origin is fairly good for the violet side of the $^2P_{1/2}$ and rather poor for the red side (does not go through origin) where corrections for non-uniformity of sensitivity are not very reliable. These considerations lead one, at least, to suspect that near the center of the lines the broadening is symmetrical for pressures below about 5 mm Hg. On the other hand the asymmetry evident in plate #92 ($^2P_{3/2}$) near the center of the line cannot conclusively be traced back to the non-uniform sensitivity of the plate. For the region occupied by this broadened line possesses a fairly uniform sensitivity. The asymmetry as the figure shows is towards the red. As already mentioned it was impossible to study the $^2P_{1/2}$ component so no conclusions can be given regarding the asymmetry. If plate #92 is significant we may conclude that the phenomenon of asymmetry sets in at about p = 10 mm. So much, then, for the region near the center of the lines.

#70
λ←

#73
← λ

#89
← λ

#92
← λ

Returning now to the extreme wings of the lines it was noticed that the irregularities in general were not situated at any particular position relative to the center of the line except for those cases to be discussed presently. In particular for plates #87 to #89 inclusive the irregularities or humps have one thing in common: they occur at wave lengths where $\frac{I}{I_o} > .90$. Also it seemed that the broader the line became the greater became the width of the hump. At relatively low pressures, see #87, it was possible to ascertain about three "humps" at the extreme wings, while at higher pressures the number of "humps" decreased to about one or two. These rather rough observations might possibly indicate a system of band-like continua whose width increases as the distance from the center increases or whose width increases because of pressure effects. For under this assumption more bands are perceptible when the lines are narrow than when the lines are wide, since the process of atomic absorption then interferes less with that of molecular absorption at lower pressures than at higher. Consequently, near the center of the line where the absorption is great the atomic absorption over shadows completely the molecular absorption. At the extreme wings the opposite would hold.

Plate #92 shows definitely a rather wide band near the wing of the line. This band has a width of about 16 Å whose center is about 45 Å away from the center of the $^2P_{3/2}$ component towards the red. #91 $^2P_{3/2}$ also shows the corresponding band. This band is by far the most pronounced. The center of the band whose width is about 20 Å on the violet side of the

$^2P_{3/2}$ (see #91) is situated about 40 Å away from the center of the doublet. Also the $^2P_{1/2}$ component seems to have a distinct band on the violet side of center of which is 40 Å away from the center of the doublet and whose width is about 20 Å. Chen[3] has observed the corresponding bands for Rb. Kuhn[65] has also observed bands in the violet side of the second doublet of the principle series of Cs and some bands for K and Na.

6. Theory versus Experiment

According to I 2 (19), (20), (21), and (22) we have according to Weiskopf, Margenau and Watson, Furrsow and Wlassow, and Professor Houston respectively, the following theoretical dependence of γ on N.

$$
\begin{array}{llll}
\text{W} & 10^7\,\gamma_1 = .37\ \text{N}, & 10^7\gamma_2 = .20\ \text{N}, & \gamma_1/\gamma_2 \cong 2\,?\ 1.85 \\
\text{M \& W} & = .79\ \text{N}, & \gamma_2 = .42\ \text{N}, & \cong 2\,?\ 1.87 \\
\text{F \& W} & = 1.32\ \text{N}, & \gamma_2 = .69\ \text{N}, & \cong 2\,?\ 1.91 \\
\text{H} & = .71\ \text{N}, & \gamma_2 = .71\ \text{N}, & = 1
\end{array}
\qquad (1)
$$

According to the results of measurement however we obtain on the average (see 4)

$$10^7\gamma_1 = 1.45\ \text{N},\ 10^7\gamma_2 = .84\ \text{N},\quad \gamma_1/\gamma_2 = 1.80 \qquad (2)$$

Comparing (1) and (2) we see that the F & W formulae are more consistent with the experimental result (2) than the others.

The form of the dependence of γ_1 on N is linear as the graph shown in Figure 4. shows. The dashed lines show the natural breadth

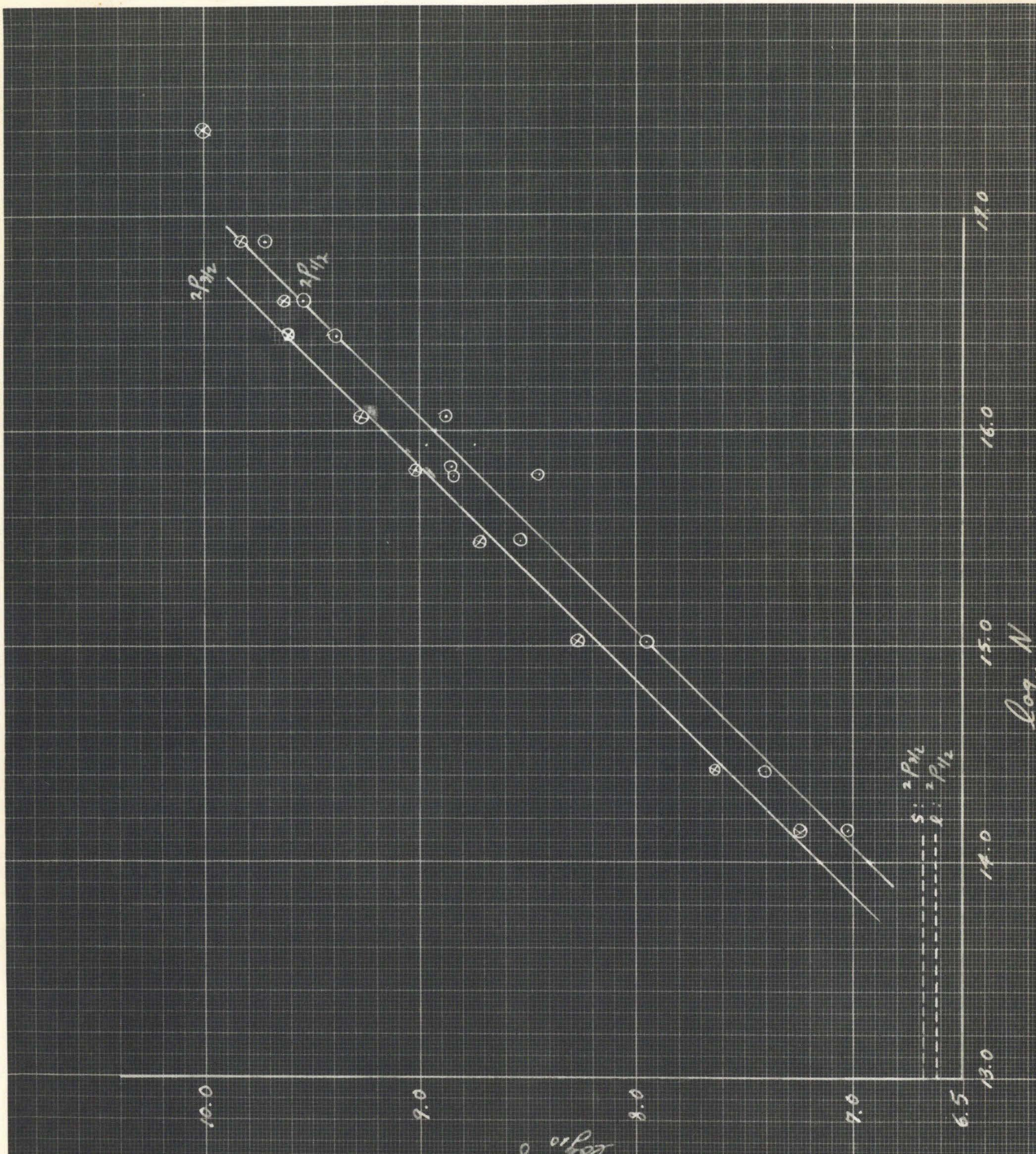

FIG. 4.

regions. Not much reliance can be put on the higher pressures (last 2 points) but are included for the sake of completeness.

On the basis of prior work on Na[2] K[1] Rb[3] we can construct the following table:

	$10^7 \gamma_1/N$	$10^7 \gamma_2/N$		
Na	1.10 (.49)	.712 (.49)	1.16	(1.00)
K	3.2 (.63)	3.2 (.63)	1.3[46]	(1.00)
Rb	.96 (.65)	.55 (.65)	1.60	(1.00)
Cs	1.45 (.71)	.84 (.71)	1.80	(1.00)

where the numbers in parentheses are the values predicted by Professor Houston. The disagreement seems to be most in the case of K. Also, there is a definite disagreement regarding the ratio γ_1/γ_2 and the table seems to show an increase with principle quantum number: 3 for Na, 4 for K, 5 for Rb, and 6 for Cs. The increase seems to be approximately .2 per qu. no.

V. Conclusion

It is not safe to say yet that errors inherent in the photographic photometry have been reduced to a minimum. The writer believes, however, that in the present investigation the method of astigmatic photometry was indispensable because of the peculiar circumstances that were present.

On the surface, at least, the dependence of γ on N seems to be more consistent with the prediction of Furssow and Wlassow than with that of the other investigators. This agreement may be accidental. It seems that more theoretical work along the lines outlined by the writer will be fruitful regarding a more accurate description of the phenomenon studied here. The program outlined, it is believed, is possible of execution.

The contours were essentially symmetrical for pressures below 10 mm Hg for the Cs vapor and the "dispersion" distribution appeared to be adequate in the description of the wings of the line, although this may be a spurious finding in view of the uncertainty due to the band-like structure appearing on the wings of the broadened lines. Indications are that above pressures of 10 mm Hg the $^2P_{3/2}$ component shows a violet asymmetry and the $^2P_{1/2}$ component a red asymmetry, although this may be due to the rather rapid variation of sensitivity of the plate especially in the region of the $^2P_{1/2}$ component as well as to the presence of the bands. The Kuhn "-3/2 law" was inadequate to describe the extreme wings of the contours.

Appendix

VI. The Rowland Grating[55]

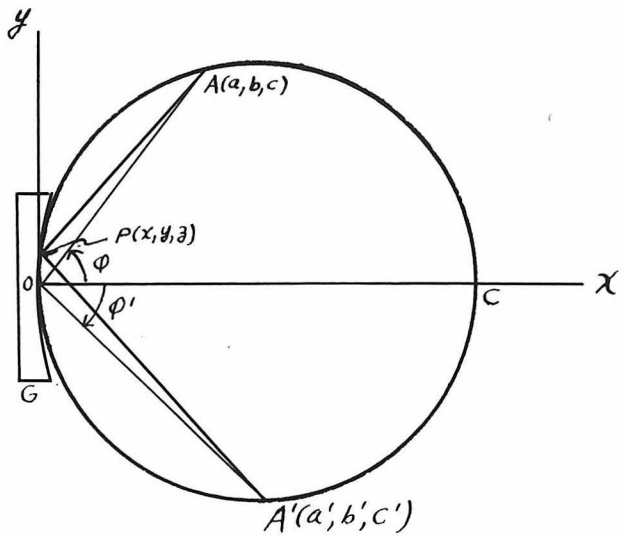

The grating G consists of a section of a spherical surface upon which are ruled furrows parallel to the yz plane which latter are a constant distance, say, e apart as measured along the y axis. The radius of the sphere is ρ . If our axes are chosen as in the figure, we may write for the grating surface the equation

$$x^2 + y^2 + z^2 - 2\rho x = 0 \qquad (1)$$

where x, y, and z are any points on the grating. Now if the points A and A' are almost in the x,y plane then the optical path from A to A' excluding second order terms is

$$AP + PA' = r + r' - \left(\frac{b}{r} + \frac{b'}{r'}\right)y - \left(\frac{c}{r} + \frac{c'}{r'}\right)z \qquad (2)$$

where $$r = \sqrt{a^2 + b^2}\ , \quad r' = \sqrt{a'^2 + b'^2} \qquad (3)$$

If second order terms are included then the optical path becomes:

$$AP + PA' = r + r' - \left(\frac{b}{r} + \frac{b'}{r'}\right)y - \left(\frac{c}{r} + \frac{c'}{r'}\right)z$$

$$+ \left[\frac{a}{2r}\left(\frac{a}{r^2} - \frac{1}{\rho}\right) + \frac{a'}{2r'}\left(\frac{a'}{r'^2} - \frac{1}{\rho}\right) + \frac{c}{2r}\left(\frac{c}{r^2} - \frac{1}{\rho}\right) +\right.$$

$$\left.\frac{c'}{2r}\left(\frac{c'}{r^2} - \frac{1}{\rho}\right)\right] y^2 -$$

$$\left(\frac{bc}{r^3} + \frac{b'c'}{r'^3}\right) yz +$$

$$\left[\frac{1}{2r}\left(1 - \frac{a}{\rho}\right) + \frac{1}{2r}\left(1 - \frac{a'}{\rho}\right) + \frac{1}{2r}\left(1 - \frac{c}{\rho}\right) + \frac{1}{2r}\left(1 - \frac{c'}{\rho}\right)\right] z^2 \qquad (4)$$

Now for $z \succeq 0$, $c \succeq 0$ the expression (2) will be constant if the zones on the grating satisfy

$$r + r' - \left(\frac{b}{r} + \frac{b'}{r'}\right) y = n\lambda \qquad (5)$$

Hence, if $\pm e$ is the interval along y from the nth to nth + 1 furrow on the grating, then

$$\left(\frac{b}{r} + \frac{b'}{r'}\right) e = \pm \lambda \qquad (6)$$

Whence we conclude that the optical path up to the first order determines the positions of the rulings of the grating in order to have A conjugate to A'. Now from (4) the path AP + PA' will be constant to terms in the second order (for $z \succeq 0$, $c \succeq 0$) if, as we see from (5) and (4), we choose

$$\left[\frac{a}{2r}\left(\frac{a}{r^2} - \frac{1}{\rho}\right) + \frac{a'}{2r'}\left(\frac{a'}{r'^2} - \frac{1}{\rho}\right)\right] = 0$$

or $$r^2 = a\rho \; ; \quad r'^2 = a'\rho \tag{7}$$

(7) then determines the Rowland circle which passes through the origin and is tangent to the y-axis having a diameter ρ . By analogy with the plane grating and from (6) A and A' are connected by

$$\left(\frac{b}{r} + \frac{b'}{r'}\right) e = m\lambda \tag{8}$$

m being the order and λ the wave length.

Now when $\frac{c}{r}$ and $\frac{c'}{r'}$ are small, a, b, a' and b' will have almost the same value as when c = c' = 0. Also A and A' will still be close to the xy plane. Thus if A moves parallel to the z axis then A' will move in the opposite direction as equation (2) shows. Hence

$$\left(\frac{\delta c}{r} = -\frac{\delta c'}{r'}\right)_{a,b,a',b',z \text{ const}} \tag{9}$$

In order to take into account the other parts of the grating which are relatively close to the xy plane we imagine the xy plane to be rotated around an axis parallel to the y-axis and passing through the point c the center of curvature of the grating so that the new position on the grating differs little from the position it formerly had. If w is the angle through which the plane is rotated A will be displaced by (ρ - a) Sin w whence from (9) A' will be displaced by $-\frac{r'}{r}$ (ρ - a)Sin w. But the process of rotation changes the (reference) position of A' by

the amount $(\rho - a')\sin w$ whence the displacement of the new position from the old is

$$\left[(\rho - a') + \frac{r'}{r}(\rho - a)\right] \sin w \qquad (10)$$

Consequently if the grating rulings have a length L along z then $\sin w \simeq \frac{L}{\rho}$, making (9) become

$$\left[(\rho - a') + \frac{r'}{r}(\rho - a)\right] \frac{L}{\rho} \qquad (11)$$

(11) shows that if the whole grating along z is utilized then every point z = c at A gives rise to a line image at A'. That is, each point at A is imaged astigmatically at A'.

Now if at A we have a slit of length s whose center is in the xy plane and is parallel to the z-axis and if the grating is uniformly reflecting then each point on the slit will give rise to a line image of length given by (11). Furthermore the end points of the slit will each give rise to an image of length (11) but the centers each will be displaced by an amount $\delta c' = + \frac{r'}{r} s$, from (9). Consequently the length of the total image will be

$$L_T = \left|\frac{r'}{r} s + \left[(\rho - a') + \frac{r'}{r}(\rho - a)\right] \frac{L}{\rho}\right| \qquad (12)$$

Now if each point on the slit emits in random phase and is uniformly illuminated then the length of the brightest part of the image will be

$$L_c = \left|\frac{r'}{r} s - \left[(\rho - a') + \frac{r'}{r}(\rho - a)\right] \frac{L}{\rho}\right| \qquad (13)$$

From the figure we have $a = r \cos \phi$, and $a' = r' \cos \phi'$ whence (12) and (13) become since from (7) $r^2 = a\varsigma$, $r'^2 = a'\varsigma$, $\frac{r'}{r} = \frac{\cos \phi'}{\cos \phi}$, hence (12) and (13) become:*

$$L_T = \frac{\cos \phi'}{\cos \phi} s + \left[\sin^2 \phi' + \sin \phi \tan \phi \cos \phi'\right] L$$

$$L = \mp \frac{\cos \phi'}{\cos \phi} s \pm \left[\sin^2 \phi' + \sin \phi \tan \phi \cos \phi'\right] L \qquad (14)$$

where the upper or lower signs are used according to whether

$$\left[\cos \phi \sin \phi' \tan \phi' + \sin^2 \phi\right] \gtrless \frac{s}{L} \qquad (15)$$

It is to be noted that the above derivation has been carried out assuming that the geometry is such as to make the point of view of geometrical optics valid. If wave optics is used the intensity distribution is essentially the same except for the points of discontinuity, which points are rounded out by diffraction effects.[6] The calculations are somewhat difficult and will not be carried out here except to point out that in principle it is only necessary to evaluate the Fresnel integral

$$I = \int_{-L/2}^{L/2} e^{\frac{2\pi i}{\lambda}(\overline{AP}+\overline{PA'})} \, dz \qquad (16)$$

where $\overline{AP} + \overline{PA'}$ is given by (4). (16) will give the intensity function due to a point source at z = c, x = a, y = b. If the slit is uniformly

* For Rowland mounting ϕ' 0.

illuminated and each point has random phase $\delta(c)$, then the resultant function will be

$$I_T = \text{const.} \int_{-L/2}^{L/2} \int_{-c/2}^{+c/2} e^{\frac{2\pi i}{\lambda}(\bar{AP}+\bar{PA'})+ \delta(c)i} \, dzdc \qquad (17)$$

The intensity at a point z = c', x = a', y = b' will then be

$$J = I_T^* \, I_T \qquad (18)$$

References and Notes

1) P. E. Lloyd, Thesis, C. I. T. (1937)

2) K. Watanabe, Thesis, C. I. T. (1940)

3) Shang-yi Ch'en, Thesis, C. I. T. (1941)

4) See 36), 9), 25) and H. Kuhn, Phil. Mag. 28, 987 (1937) for example

5) G. H. Dieke, J. O. S. A. 23, 280 (1933)

6) M. I. Bresch, J. O. S. A. 28, 493 (1938)

7) Dirac, Quantum Mechanics

8) W. E. Forsythe, Measurement of Radiant Energy, p. 19, Mc Graw-Hill Book Co. 1937

9) H. Margenau & W. W. Watson, Rev. of Mod. Phys. 8, 28 (1936)

10) C. Fuchtbauer & F. Gossler, Zeits. f. Phys. 87, 89 (1933)
H. Margenau & W. W. Watson, Phys. Rev. 44, 92 (1933)

11) R. C. Tolman, Phys. Rev. 23, 609 (1924)

12) R. Ladenburg, Zeits. f. Phys. 4, 451 (1921)
R. Ladenburg & F. Reiche, Nature 11, 596 (1923)

13) S. A. Korff & G. Breit, Rev. Mod. Phys. 4, 471 (1932)

14) Heitler, Quant. Theory of Radiation, p. 34, Oxford 1936

15) " " " " " p. 35,36 " "

16) This follows from Kerchoff's law

17) Weiskopf & Wigner, Zeits. f. Phys. 63, 14 (1930)
" " " " " " 65, 18 (1930)

18) Hoyt, Phys. Rev. 36, 860 (1931)

19) See Mitchell and Zemansky's text, 63)

20) This nomer is a hangover from the old Lorentz theory

21) A. Jablonski, Zeits. f. Phys. 70, 723 (1931)

22) H. Margenau, Phys. Rev. 40, 387 (1932)

" " " " 43, 129 (1933)

23) Kulp, Zeits. f. Phys. 79, 495 (1933)

24) H. Margenau & W. W. Watson, Phys. Rev. 44 (1933)

25) Weiskopf, Phys. Zeits, 34, 1 (1933)

26) R. Minkowski, Zeits. f. Phys. 55, 16 (1929)

27) O. Oldenburg, Zeits. f. Phys. 51, 605 (1928)

28) W. Lenz, Zeits. f. Phys. 25, 299 (1924)

29) V. Weisskopf, Phys. Zeits. 34, 15 (1933)

30) J. Holztmark, Zeits. f. Phys. 34, 722 (1925)

31) W. Shutz & L. Mensing, Zeits. f. Phys. 61, 655 (1930)

32) See 25), p. 20

33) V. Weiskopf, Zeits. f. Phys. 75, 287 (1932)

34) See 9), p. 22

35) Furrsow & Wlassow, Phys. Zeits. & Sowjet Union, 10, 378 (1936)

36) W. V. Houston, Phys. Rev. 54, 888 (1938)

37) Condon & Shortley, Theory of Atomic Spectra, p. 98, Cambridge (1935)

38) H. Kuhn, Phil. Mag. 18, 987 (1934)

See also 9)

39) See 25), 8) and 3) for example

40) R. Minkowski, Zeits. f. Phys. 36, 839 (1926)

41) S. A. Korff, Astrophys. J. 76, 124 (1932)
Phys. Rev. 38, 477 (1931)

42) M. Weingeroff, Zeits. f. Phys. 67, 679 (1931)

43) W. Schutz, Zeits. f. Phys. 45, 30 (1927)

44) A. Unsold, Zeits. f. Astrophy. 2, 199 (1931)

45) See 43), also
G. R. Harrison & J. C. Slater, Phys. Rev. 26, 176 (1925)
G. R. Harrison, Phys. Rev. 25, 168 (1925)
B. Trumpy, Zeits. f. Phys. 34, 715 (1925)
" " " " " 40, 594 (1926)
F. Waibel, " " " 53, 459 (1929)

46) Lloyd originally obtained 1.05 for the ratio, but rough measurements of Prof. Bowen indicated that it was 1.3 or 1.4. This discrepancy of Lloyd's is probably due to the non-uniform characteristics of the plates he used.

47) A. Jablonski, Acta Phys. Polonica VI-4, 371 (1937)
" " " " " VII-2, 196 (1938)

48) Tolman's book was used as a reference throughout:
The Principles of Statistical Mechanics, Oxford (1938)

49) I am indebted to Prof. Houston for recalling this fact to the writer.

50) See any text book on quantum mechanics or notes on the subject by Prof. Houston or Prof. Epstein

51) See 48)

52) See 48), p. 447

53) R. T. Brice, Thesis, C. I. T. (1936)

Strong & Brice, J. O. S. A. 25, 207 (1935)

54) See Statistics Notes (Unpublished) by Dr. Dinsmore Alter of the Institute staff

55) See Mack, Stehen, and Edlen, J. O. S. A. 22, 245 (1933) for a comprehensive study of the Rowland grating. An adequate elementary theory is given in Kayser, Handbuch der Spectroscopy VI, p. 450-64.

56) J. H. Webb, J. O. S. A. 23, 157 (1933)

57) E. R. Bullock, Sci. Ind. Phot. Series II, 1,124,169,321,366 (1930)

58) See 5), p. 280.

59) I. M. Mathews, Proc. Roy. Soc. A 120, 650 (1938)

60) J. B. Taylor & I. Langmuir, Phys. Rev. 51, 753 (1937)

61) R. Ladenburg & F. Reiche, Ann. d. Phys. 42, 181 (1913)

62) R. Minkowski, Zeit. f. Phys. 36, 839 (1926)

63) Resonance Radiation and Lifetime of Excited States, Mitchell & Zemansky, p. 146-7

64) See I-2, (9)

65) H. Kuhn, Zeit. f. Phys. 76, 782 (1932)